Journal of Industrial and Management Optimization

https://www.aimspress.com/journal/jimo

JIMO, 22(12): 6668–6708.
DOI:10.3934/jimo.2026223
Received: 29 September 2026
Revised: 10 November 2026
Accepted: 11 November 2026
Published: 19 November 2026

Research article

Random-risk-aversion pension investment under correlated Heston–CIR dynamics

Yang Jiang[1], **Yong He**[2,*] **and Yulei Chen**[2]

[1] School of Marxism, Southwestern University of Finance and Economics, Chengdu 611130, China

[2] School of Mathematical Sciences, Chongqing University of Science and Technology, Chongqing 401331, China

* **Correspondence:** Email: 2007046@cqust.edu.cn.

Abstract: We study time-consistent investment for a protected defined contribution pension plan with random relative risk aversion in a correlated Heston–Cox–Ingersoll–Ross (CIR) market. The framework combines stochastic contributions, inflation, an inflation-linked life annuity guarantee, Heston variance, and a CIR short rate. Under an imposed common $\sqrt{V_t}$ local spanning structure for the inflation and contribution loadings, the contribution and guarantee claims are replicated with a stock, a nominal bond, and an indexed bond before the pension account is reduced to real auxiliary wealth. This replication and the reduction in protected wealth are conditional on that structure, while the variance component driven by W_3 remains unspanned. A monetary certainty-equivalent criterion and spike deviation analysis conditionally verify an equilibrium continuation system and its feedback strategy. For a general risk aversion distribution, the aggregate feedback satisfies a fixed-point condition rather than an existence result; local classical existence is established only for the finite two-point system on a stopped positive state rectangle. For a degenerate risk aversion distribution, variance–rate correlation generates a $\sqrt{vr}$ term that precludes the standard affine Riccati ansatz under the stated nondegeneracy conditions. The numerical parameter studies use specified model inputs rather than a data calibration. They show that the preference dispersion changes effective risk aversion and portfolio exposures, while variance–rate dependence changes nominal bond hedging. The resulting strategy supplies stock, nominal bond, indexed bond, and cash allocations for the protected pension account.

Keywords: defined contribution pension plan; random risk aversion; expected certainty equivalent; Heston stochastic volatility; CIR interest rate; variance–rate correlation; equilibrium control
Mathematics Subject Classification: 91G10, 91G80, 93E20

1. Introduction

Retirement security is both a long-horizon financial problem and a component of social protection. For workers, pension income sustains material conditions after wage earnings cease. On this basis, old age protection can be interpreted in Marxist political economy as part of the social reproduction of labor power across the life course [1–3]. This interpretation is also consistent with Marx's discussion of prior deductions from the total social product: Before the means of consumption are distributed to individuals, resources are set aside for common needs and for people unable to work [4]. A pension arrangement, therefore, does more than organize individual savings; it also allocates the costs and risks of retirement among workers, employers, financial markets, and the state. This institutional role is relevant to Chinese modernization, which emphasizes people-centered development, common prosperity, and an equitable and sustainable social security system. Because defined contribution arrangements invest long-term savings in capital markets, they create a central design question: How can market-based accumulation remain compatible with livelihood protection and sustainable retirement security?

This design question becomes concrete in the allocation of retirement risks between a plan's sponsors and members. Defined benefit and defined contribution (DC) plans allocate these risks differently. In a DC plan, members bear most of the investment and longevity risk, so contribution allocation over a long accumulation horizon directly affects their attainable retirement income. Minimum guarantees limit downside exposure but convert portfolio choice into an asset–liability problem. Continuous-time studies therefore connect terminal protection with optimal investment [5, 6], stochastic contributions and inflation-indexed securities [7], and life annuity conversion guarantees [8, 9]. These mechanisms translate broad retirement protection objectives into pension account design.

The political economy literature clarifies why these risk transfers matter beyond portfolios' performance. Pension systems distribute both retirement income and exposure to uncertainty, while public and occupational arrangements mediate relations among labor, capital, and the state across the life course [2]. The expansion of funded pensions also places deferred retirement resources within financial markets. This process creates opportunities for long-term accumulation, but it exposes retirement provision to market volatility and financial intermediation [10–12]. A shift toward individual accounts can consequently transfer more investment and longevity risk to workers and households. In China, expanded pension coverage has strengthened old age protection, while differences in participation, contribution capacity, and benefit entitlement continue to raise questions of equality and integration [13]. Although this literature does not determine an optimal portfolio, it provides the institutional motivation for guarantees and risk-sensitive DC allocation.

Stochastic investment opportunities are especially relevant over pension horizons. The Heston model represents mean-reverting variance and return–variance dependence [14], while the Cox–Ingersoll–Ross (CIR) model supplies a positive affine short rate and tractable bond prices [15]. Sun et al. [16] derived mean–variance equilibrium strategies for a DC plan with inflation, stochastic income, and Heston volatility. Guan and Liang [17] combined Heston volatility with affine stochastic rates, stochastic contributions, and a retirement guarantee under constant relative risk aversion (CRRA) utility. Zhang et al. [18] instead derived a time-consistent mean–variance equilibrium when both the interest rate and volatility are stochastic. Related robust formulations have studied ambiguity aversion in the same two-factor pension setting [19]. Together, these studies show that stochastic factor dynamics determine

intertemporal hedging demands in DC investment, but they retain a fixed preference parameter or a mean–variance criterion rather than monetary aggregation over random risk aversion.

Dependence between stochastic variance and interest rates adds a further dimension to long-horizon asset allocation. Grzelak and Oosterlee [20] examined Heston models with Hull–White or CIR rates and developed affine approximations for derivative pricing under nonzero factor correlation. Ascione et al. [21] use a correlated four-factor Heston–CIR model with Lévy dynamics for foreign exchange option pricing. These studies established hybrid stochastic volatility and stochastic rate modeling benchmarks, but their objective is derivative pricing rather than pension control or random preference equilibrium. Ballestra et al. [22] documented time variation in the relation between equity volatility and interest rate movements. This literature motivates a correlated factor treatment for pension investment, where the joint dynamics must be considered together with liability replication and time-consistent decision-making.

Risk preference uncertainty is a separate source of time inconsistency. A single relative risk aversion coefficient is difficult to elicit, and estimates differ across members and methods [23–25]. A direct weighted sum of utilities is scale-dependent. Desmettre and Steffensen [26] instead transformed each conditional expected utility into its monetary certainty equivalent and then averaged monetary quantities. The criterion is economically comparable across risk aversion states but violates the dynamic programming principle. Equilibrium is therefore defined through local deviations in the Markovian game framework [27, 28]. Wang and Jia [29] applied this framework to a protected DC plan with stochastic contributions and inflation. They transformed the non-self-financing account into an auxiliary problem and derived equilibrium strategies under constant stock volatility and a constant nominal rate.

Against this background, political economy and mathematical finance address complementary levels of the pension problem. Political economy examines how retirement risks are allocated among institutions and social groups. Mathematical finance studies how specified risks can be priced, hedged, and dynamically managed. The present paper works mainly at the second level, while using the first to motivate and interpret the guarantee design and preference heterogeneity. It does not model class structure, income redistribution, or the overall effectiveness of China's pension institutions. Accordingly, Table 1 summarizes the mathematical and actuarial studies that provide the model's direct technical foundations.

The comparison distinguishes the relevant strands. Guan and Liang [17] addressed protected DC investment under Heston volatility and stochastic rates with fixed CRRA preferences, while Zhang et al. [18] obtained a time-consistent mean–variance equilibrium under stochastic interest rates and volatility. Correlated Heston rate studies have concentrated on pricing and approximation questions [20, 21]. Together, these comparisons locate the present gap at the intersection of protected pension liabilities, random preference aggregation, stochastic volatility, stochastic interest rates, and local deviation equilibrium.

This paper develops such a treatment in continuous time. It extends the protected account reduction and monetary certainty-equivalent equilibrium framework of Wang and Jia [29] to a correlated Heston–CIR market. The Heston–CIR specification supplies the market setting. The primary theoretical contribution identifies the scope of the standard affine reduction when variance and rates are correlated, while the corresponding economic contribution recovers the correlation-induced nominal bond hedge within the protected account equilibrium. The analysis also maps the equilibrium policy into allocations among traded pension assets.

The remainder of this paper is organized as follows. Section 2 formulates the market and pension problem. Section 3 gives the auxiliary reduction and verification theorem. Section 4 derives the general,

two-point, and degenerate cases. Section 5 reports the numerical and welfare analyses. Section 6 concludes the paper.

Table 1. Comparison of pension protection, preference criteria, and market factors in the related literature and the present model.

Study	Pension protection	Preference criterion	Market factors	Role in the present paper
Boulier et al. [5]	Protected DC fund	Fixed preferences	Stochastic interest rate	Early protected pension asset–liability framework
Guan and Liang [17]	Contributions and retirement guarantee	CRRA utility	Heston volatility and affine rates	Stochastic factor pension benchmark
Sun et al. [16]	DC income and inflation features	Mean–variance equilibrium	Heston volatility	Heston equilibrium hedging in a pension setting
Zhang et al. [18]	DC investment	Time-consistent equilibrium	Stochastic rates and volatility	Equilibrium under two stochastic investment factors
Desmettre and Steffensen [26]	–	Monetary aggregation of random risk aversion	General investment setting	Certainty equivalent preference aggregation
Wang and Jia [29]	Contributions and annuity guarantee	Random risk aversion equilibrium	Constant stock volatility and nominal rate	Objective, replication sequence, and local deviation architecture
Grzelak and Oosterlee [20]	–	Pricing	Correlated Heston and stochastic rate models	Correlated factor tractability benchmark
Ascione et al. [21]	–	Pricing	Correlated Heston–CIR–Lévy foreign exchange model	Heston–CIR application outside pension control
Present paper	Contributions and annuity guarantee	Random risk aversion equilibrium	Exact correlated Heston–CIR state dynamics	Protected account equilibrium with random preferences and correlated market factors

2. Problem formulation

Let $(\Omega, \mathcal{F}, \{\mathcal{F}_t\}_{0\le t\le T}, \mathbb{P})$ satisfy the usual conditions and support four independent Brownian motions W_1, W_2, W_3, W_4. The shocks W_1, W_2, W_4 are traded; W_3 is the residual variance shock. Dependence between variance and the short rate is generated by loading variance on the traded rate shock W_4. All

processes are adapted and sufficiently integrable. We write $\mathbb{E}_t[\cdot] = \mathbb{E}^{\mathbb{P}}[\cdot \mid \mathcal{F}_t]$ and $\mathbb{E}_t^{\mathbb{Q}}$ analogously. For a function of (t, z, v, r), $C^{1,2,2,2}$ denotes one continuous derivative in time and two continuous derivatives in each state variable, including the mixed derivatives used below; $C^{1,2,2}$ has the analogous meaning for functions of (t, v, r).

2.1. The financial market

The money market account satisfies

$$\frac{\mathrm{d}S_0(t)}{S_0(t)} = r_t \,\mathrm{d}t. \tag{1}$$

The Heston stock price is introduced as follows:

$$\frac{\mathrm{d}S_t}{S_t} = (r_t + \lambda_S V_t)\,\mathrm{d}t + \sqrt{V_t}\,\mathrm{d}W_1(t). \tag{2}$$

Its instantaneous variance is the square-root process

$$\mathrm{d}V_t = \kappa_v(\theta_v - V_t)\,\mathrm{d}t + \sigma_v\sqrt{V_t}\{\rho\,\mathrm{d}W_1(t) + \chi\,\mathrm{d}W_4(t) + \sqrt{1-\rho^2-\chi^2}\,\mathrm{d}W_3(t)\}. \tag{3}$$

Thus the instantaneous market price of the traded W_1 risk is $\lambda_S\sqrt{V_t}$, while the W_3 component is not spanned. The nominal short rate follows the CIR process

$$\mathrm{d}r_t = \kappa_r(\theta_r - r_t)\,\mathrm{d}t + \sigma_r\sqrt{r_t}\,\mathrm{d}W_4(t). \tag{4}$$

The parameter ρ is the return–variance correlation and χ is the variance–rate correlation, because

$$\mathrm{d}\langle V, r\rangle_t = \chi\sigma_v\sigma_r\sqrt{V_t r_t}\,\mathrm{d}t. \tag{5}$$

We assume $r_0, V_0 > 0$, positive mean-reversion parameters,

$$\rho^2 + \chi^2 < 1, \tag{6}$$

and

$$2\kappa_r\theta_r \geq \sigma_r^2, \qquad 2\kappa_v\theta_v \geq \sigma_v^2, \tag{7}$$

which are the Feller conditions used below. The nominal price level is the Heston analog of the two-shock inflation process in the benchmark:

$$\frac{\mathrm{d}P_t}{P_t} = [\eta + \sigma_{P1}\lambda_S V_t + \sigma_{P2}\lambda_p]\,\mathrm{d}t + \sigma_{P1}\sqrt{V_t}\,\mathrm{d}W_1(t) + \sigma_{P2}\,\mathrm{d}W_2(t). \tag{8}$$

The drift compensators preserve the benchmark pricing drift η after the traded risk premia are removed.

Define the minimal martingale measure $\mathbb{Q}$ by

$$\left.\frac{\mathrm{d}\mathbb{Q}}{\mathrm{d}\mathbb{P}}\right|_{\mathcal{F}_T} = \mathcal{E}\left(-\int_0^T \lambda_S\sqrt{V_s}\,\mathrm{d}W_1(s) - \int_0^T \lambda_p\,\mathrm{d}W_2(s) - \int_0^T \lambda_r\sqrt{r_s}\,\mathrm{d}W_4(s)\right), \tag{9}$$

and assume that this stochastic exponential is a true martingale. Then

$$\mathrm{d}W_1^{\mathbb{Q}} = \mathrm{d}W_1 + \lambda_S \sqrt{V}\,\mathrm{d}t, \qquad \mathrm{d}W_2^{\mathbb{Q}} = \mathrm{d}W_2 + \lambda_p\,\mathrm{d}t, \qquad \mathrm{d}W_4^{\mathbb{Q}} = \mathrm{d}W_4 + \lambda_r \sqrt{r}\,\mathrm{d}t, \tag{10}$$

while W_3 is unchanged. Consequently, the stock has drift r_t under $\mathbb{Q}$, and the state variables satisfy

$$\frac{\mathrm{d}S_t}{S_t} = r_t\,\mathrm{d}t + \sqrt{V_t}\,\mathrm{d}W_1^{\mathbb{Q}}(t), \tag{11}$$

$$\begin{aligned}\mathrm{d}V_t = {} & [\kappa_v\theta_v - (\kappa_v + \rho\sigma_v\lambda_S)V_t - \chi\sigma_v\lambda_r\sqrt{V_t r_t}]\,\mathrm{d}t \\ & + \sigma_v\sqrt{V_t}\{\rho\,\mathrm{d}W_1^{\mathbb{Q}} + \chi\,\mathrm{d}W_4^{\mathbb{Q}} + \sqrt{1-\rho^2-\chi^2}\,\mathrm{d}W_3\},\end{aligned} \tag{12}$$

$$\mathrm{d}r_t = [\kappa_r\theta_r - (\kappa_r + \sigma_r\lambda_r)r_t]\,\mathrm{d}t + \sigma_r\sqrt{r_t}\,\mathrm{d}W_4^{\mathbb{Q}}(t), \tag{13}$$

$$\frac{\mathrm{d}P_t}{P_t} = \eta\,\mathrm{d}t + \sigma_{P1}\sqrt{V_t}\,\mathrm{d}W_1^{\mathbb{Q}}(t) + \sigma_{P2}\,\mathrm{d}W_2^{\mathbb{Q}}(t). \tag{14}$$

Put $\bar{\kappa}_r = \kappa_r + \sigma_r\lambda_r$ and let τ denote the time to maturity.

Proposition 1. *The time t price of a nominal zero-coupon bond maturing at T_b is*

$$N(t, T_b) = A_N(\tau)e^{-B_N(\tau)r_t}, \qquad \tau = T_b - t, \tag{15}$$

where

$$B_N' = 1 - \bar{\kappa}_r B_N - \tfrac{1}{2}\sigma_r^2 B_N^2, \qquad B_N(0) = 0, \tag{16}$$

$$\frac{A_N'}{A_N} = -\kappa_r\theta_r B_N, \qquad A_N(0) = 1. \tag{17}$$

The price of a zero-coupon indexed bond paying P_{T_b} is

$$I(t, T_b) = P_t e^{\eta\tau}A_N(\tau)e^{-B_N(\tau)r_t}. \tag{18}$$

For self-financing rolling bonds with constant remaining maturities K_N and K_I, their instantaneous rate loadings are

$$b_N = -\sigma_r B_N(K_N), \qquad b_I = -\sigma_r B_N(K_I). \tag{19}$$

In particular, $b_I = b_N$ when the two rolling bonds have the same remaining maturity.

Proof. Under $\mathbb{Q}$, the short-rate drift in (13) is $\kappa_r\theta_r - \bar{\kappa}_r r$. For a fixed maturity T_b, the nominal bond price $N(t, r; T_b)$ therefore solves

$$N_t + (\kappa_r\theta_r - \bar{\kappa}_r r)N_r + \tfrac{1}{2}\sigma_r^2 r N_{rr} - rN = 0, \qquad N(T_b, r; T_b) = 1. \tag{20}$$

Set $\tau = T_b - t$ and substitute $N = A_N(\tau)e^{-B_N(\tau)r}$. The required derivatives are

$$N_t = -\left(\frac{A_N'}{A_N} - B_N' r\right)N, \qquad N_r = -B_N N, \qquad N_{rr} = B_N^2 N. \tag{21}$$

After division by N, the constant and r coefficients in (20) are

$$-\frac{A_N'}{A_N} - \kappa_r\theta_r B_N = 0, \tag{22}$$

$$B_N' + \bar{\kappa}_r B_N + \tfrac{1}{2}\sigma_r^2 B_N^2 - 1 = 0. \tag{23}$$

These are (17)–(16). If $d_r = (\bar{\kappa}_r^2 + 2\sigma_r^2)^{1/2}$, their explicit solution is

$$B_N(\tau) = \frac{2(e^{d_r\tau} - 1)}{(d_r + \bar{\kappa}_r)(e^{d_r\tau} - 1) + 2d_r}, \tag{24}$$

$$A_N(\tau) = \left[\frac{2d_r e^{(\bar{\kappa}_r + d_r)\tau/2}}{(d_r + \bar{\kappa}_r)(e^{d_r\tau} - 1) + 2d_r}\right]^{2\kappa_r\theta_r/\sigma_r^2}. \tag{25}$$

Itô's formula and (20) give

$$\frac{\mathrm{d}N(t, T_b)}{N(t, T_b)} = r_t\,\mathrm{d}t - \sigma_r B_N(\tau)\sqrt{r_t}\,\mathrm{d}W_4^{\mathbb{Q}}(t). \tag{26}$$

Using $\mathrm{d}W_4^{\mathbb{Q}} = \mathrm{d}W_4 + \lambda_r\sqrt{r}\,\mathrm{d}t$ and setting $\tau = K_N$ yields (29) with $b_N = -\sigma_r B_N(K_N)$.

Let $J(t, p, v, r; T_b)$ be the price of the claim P_{T_b}. Its full pricing partial differential equation (PDE) contains the (P, V) covariance term because the same $W_1^{\mathbb{Q}}$ drives both processes and the (V, r) covariance term because of χ. The affine candidate below is linear in p and independent of v, so $J_{pp} = J_v = J_{vv} = J_{pv} = J_{vr} = 0$. The PDE therefore reduces exactly to

$$J_t + \eta p J_p + (\kappa_r\theta_r - \bar{\kappa}_r r)J_r + \tfrac{1}{2}\sigma_r^2 r J_{rr} - rJ = 0, \qquad J(T_b, p, v, r; T_b) = p. \tag{27}$$

Direct substitution shows that $J = pe^{\eta\tau}A_N(\tau)e^{-B_N(\tau)r}$ solves this equation. Its relative $\mathbb{Q}$-diffusion vector is

$$(\sigma_{P1}\sqrt{v},\ \sigma_{P2},\ -\sigma_r B_N(\tau)\sqrt{r})^\top. \tag{28}$$

Because a correctly priced traded claim has $\mathbb{Q}$-drift r, conversion back to $\mathbb{P}$ adds the inner product of this vector with $\vartheta = (\lambda_S\sqrt{v}, \lambda_p, \lambda_r\sqrt{r})^\top$. Evaluating at $\tau = K_I$ gives (30) and $b_I = -\sigma_r B_N(K_I)$. Finally, setting $t = T$ and $T_b = s$ in (18) and then inserting (33) into (34) gives (35)–(36).

The physical return equations are therefore

$$\frac{\mathrm{d}B_t^N}{B_t^N} = [r_t + b_N(t)\lambda_r r_t]\,\mathrm{d}t + b_N(t)\sqrt{r_t}\,\mathrm{d}W_4(t), \tag{29}$$

$$\begin{aligned}\frac{\mathrm{d}B_t^I}{B_t^I} &= [r_t + \sigma_{P1}\lambda_S V_t + \sigma_{P2}\lambda_p + b_I(t)\lambda_r r_t]\,\mathrm{d}t \\ &\quad + \sigma_{P1}\sqrt{V_t}\,\mathrm{d}W_1(t) + \sigma_{P2}\,\mathrm{d}W_2(t) + b_I(t)\sqrt{r_t}\,\mathrm{d}W_4(t).\end{aligned} \tag{30}$$

We retain the notation $b_N(t), b_I(t)$ to allow deterministic maturity schedules; for constant maturity rolls the quantities in (19) are constant. Below we require bounded b_N, b_I, and $b_N \neq 0$.

For risky assets ordered as (S, B^N, B^I) and traded shocks ordered as (W_1, W_2, W_4), the exposure matrix is

$$L(t, v, r) = \begin{pmatrix} \sqrt{v} & 0 & \sigma_{P1}\sqrt{v} \\ 0 & 0 & \sigma_{P2} \\ 0 & b_N(t)\sqrt{r} & b_I(t)\sqrt{r} \end{pmatrix}. \tag{31}$$

It is invertible for $v, r > 0$. Thus every claim driven only by (W_1, W_2, W_4) is locally spanned, whereas the W_3 driven idiosyncratic component of the variance process remains unspanned. The additional W_4 loading in (3) does not enlarge the traded shock dimension; it changes the intertemporal hedge against variance because the rate asset now partly spans variance risk.

2.2. Stochastic contribution and annuity guarantee

The contribution rate preserves the two benchmark shocks, with its stock-driven loading scaled by Heston volatility.

$$\frac{\mathrm{d}C_t}{C_t} = [\mu + \sigma_{C1}\lambda_S V_t + \sigma_{C2}\lambda_p]\,\mathrm{d}t + \sigma_{C1}\sqrt{V_t}\,\mathrm{d}W_1(t) + \sigma_{C2}\,\mathrm{d}W_2(t). \tag{32}$$

Under $\mathbb{Q}$, its drift is μ. The coefficients $\sigma_{C1}, \sigma_{C2} > 0$ have the same roles as in the benchmark.

The common $\sqrt{V_t}$ scaling in (8) and (32) is imposed as a structural local spanning assumption. It makes the W_1 shocks of the price level and contribution claims proportional to the stock loading, while their W_2 shocks are carried by the indexed bond. The claims are consequently spanned by the three traded directions in (31). This is a model specification for claim replication rather than a microfounded equation for wage growth or price inflation. The W_3 component of the variance state remains unspanned, so the factor market is not completed by this assumption. Accordingly, exact three-asset replication and the resulting reduction in protected wealth are conditional on the common loading structure specified above.

At retirement T, the member purchases a real life annuity. Let $a(s) = a(T)e^{a_0(s-T)}$ for $s \in [T, \omega]$. Under the Abraham De Moivre law

$${}_{s-T}p_T = \exp\left(-\int_T^s \frac{1}{\omega - u}\,\mathrm{d}u\right) = \frac{\omega - s}{\omega - T}. \tag{33}$$

If $I(T, s)$ is the time T price of one unit of P_s, the nominal guarantee is

$$G_T = \int_T^\omega a(s) I(T, s)\,{}_{s-T}p_T\,\mathrm{d}s = P_T\,\mathfrak{a}(r_T), \tag{34}$$

where Proposition 1 gives

$$I(T, s) = P_T e^{\eta(s-T)} A_N(s - T) e^{-B_N(s-T)r_T}, \tag{35}$$

$$\mathfrak{a}(r) = \int_T^\omega a(s) e^{\eta(s-T)} A_N(s - T) e^{-B_N(s-T)r} \frac{\omega - s}{\omega - T}\,\mathrm{d}s. \tag{36}$$

The CIR annuity factor is positive and smooth because the integration interval is finite and the affine bond coefficients are smooth.

2.3. The optimization problem

Let $\pi = (\pi_S, \pi_N, \pi_I)^\top$ denote pension account fractions in the stock, nominal bond, and indexed bond; cash is the residual. With

$$\vartheta(v, r) = (\lambda_S\sqrt{v}, \lambda_p, \lambda_r\sqrt{r})^\top, \tag{37}$$

the nominal pension wealth satisfies

$$\mathrm{d}X_t = [r_t X_t + X_t \pi_t^\top L(t, V_t, r_t)^\top \vartheta(V_t, r_t) + C_t]\,\mathrm{d}t + X_t \pi_t^\top L(t, V_t, r_t)^\top\,\mathrm{d}W_t, \tag{38}$$

where $W = (W_1, W_2, W_4)^\top$. The terminal real surplus is $(X_T - G_T)/P_T$ and is required to be positive.

Let γ be a positive bounded random variable, independent of the Brownian motions, with the distribution Γ supported in a compact subset of $(0,\infty)\setminus\{1\}$. For power utility

$$u^\gamma(z)=\frac{z^{1-\gamma}}{1-\gamma},\qquad z>0. \tag{39}$$

The expected certainty equivalent objective is

$$V_1(t,x,p,c,v,r)=\sup_\pi \int (u^\gamma)^{-1}\left(\mathbb{E}_{t,x,p,c,v,r}\left[u^\gamma\left(\frac{X_T^\pi-G_T}{P_T}\right)\right]\right)\mathrm{d}\Gamma(\gamma). \tag{40}$$

The inverse utility converts each conditional expected utility into money before aggregation. A direct average of utilities would instead combine quantities with incompatible affine scales. The certainty-equivalent criterion is time-inconsistent because future selves recompute the conditional expectations inside the nonlinear inverses.

Definition 1. *A feedback strategy π is admissible if it is progressively measurable and continuous in its state arguments. Equation* (38) *has a unique strong solution, $X_T > G_T$ almost surely, the stochastic integrals used below are true martingales after localization, and the integral in* (40) *is finite.*

3. Problem reduction and verification theorem

3.1. An auxiliary problem

For $t\le s\le T$, introduce a hypothetical derivative paying C_s at s as follows:

$$D(t,s)=\mathbb{E}_t^{\mathbb{Q}}\left[e^{-\int_t^s r_u\,\mathrm{d}u}C_s\right]=C_t d(t,s,r_t). \tag{41}$$

The Feynman–Kac formula gives

$$\begin{aligned}0&=d_t+[\kappa_r\theta_r-(\kappa_r+\sigma_r\lambda_r)r]d_r+\tfrac{1}{2}\sigma_r^2 r d_{rr}+(\mu-r)d,\\ d(s,s,r)&=1.\end{aligned} \tag{42}$$

The present value of contributions is

$$F(t,T)=\int_t^T D(t,s)\,\mathrm{d}s=C_t f(t,r_t),\qquad f(t,r)=\int_t^T d(t,s,r)\,\mathrm{d}s, \tag{43}$$

where

$$0=f_t+[\kappa_r\theta_r-(\kappa_r+\sigma_r\lambda_r)r]f_r+\tfrac{1}{2}\sigma_r^2 r f_{rr}+(\mu-r)f+1,\qquad f(T,r)=0. \tag{44}$$

The time t value of the guarantee is

$$G(t)=\mathbb{E}_t^{\mathbb{Q}}\left[e^{-\int_t^T r_u\,\mathrm{d}u}G_T\right]=P_t q(t,r_t), \tag{45}$$

and q solves

$$0=q_t+[\kappa_r\theta_r-(\kappa_r+\sigma_r\lambda_r)r]q_r+\tfrac{1}{2}\sigma_r^2 r q_{rr}+(\eta-r)q,\qquad q(T,r)=\mathfrak{a}(r). \tag{46}$$

Proposition 2. *The ex-dividend contribution value F is replicated by the fractions*

$$\pi_I^F = \frac{\sigma_{C2}}{\sigma_{P2}}, \qquad \pi_S^F = \sigma_{C1} - \frac{\sigma_{P1}\sigma_{C2}}{\sigma_{P2}}, \qquad \pi_N^F = \frac{\sigma_r f_r/f - b_I \pi_I^F}{b_N}. \tag{47}$$

The guarantee value G is replicated by

$$\pi_I^G = 1, \qquad \pi_S^G = 0, \qquad \pi_N^G = \frac{\sigma_r q_r/q - b_I}{b_N}. \tag{48}$$

In particular, we have

$$\mathrm{d}F_t = [r_t F_t - C_t + F_t(\alpha_t^F)^\top \vartheta_t]\,\mathrm{d}t + F_t(\alpha_t^F)^\top \mathrm{d}W_t, \tag{49}$$
$$\mathrm{d}G_t = [r_t G_t + G_t(\alpha_t^G)^\top \vartheta_t]\,\mathrm{d}t + G_t(\alpha_t^G)^\top \mathrm{d}W_t, \tag{50}$$

where $\alpha^F = L\pi^F$ and $\alpha^G = L\pi^G$.

Proof. We give the calculation in four steps.

Step 1: Contribution value. Under $\mathbb{Q}$,

$$\frac{\mathrm{d}C_t}{C_t} = \mu\,\mathrm{d}t + \sigma_{C1}\sqrt{V_t}\,\mathrm{d}W_1^{\mathbb{Q}}(t) + \sigma_{C2}\,\mathrm{d}W_2^{\mathbb{Q}}(t). \tag{51}$$

First, verify the PDE for the aggregate contribution value. From $f(t,r) = \int_t^T d(t,s,r)\,\mathrm{d}s$ and $d(t,t,r) = 1$, Leibniz's rule gives

$$f_t = -1 + \int_t^T d_t(t,s,r)\,\mathrm{d}s, \qquad f_r = \int_t^T d_r(t,s,r)\,\mathrm{d}s, \qquad f_{rr} = \int_t^T d_{rr}(t,s,r)\,\mathrm{d}s. \tag{52}$$

Integrating (42) over $s \in [t,T]$ and inserting these identities yields (44), including the source term $+1$ and the terminal condition $f(T,r) = 0$.

For $F(t,c,r) = cf(t,r)$, we have

$$F_c = f, \quad F_r = cf_r, \quad F_{cc} = 0, \quad F_{cr} = 0, \quad F_{rr} = cf_{rr}. \tag{53}$$

The $\mathbb{Q}$-drift from Itô's formula is

$$c\{f_t + \mu f + [\kappa_r\theta_r - (\kappa_r + \sigma_r\lambda_r)r]f_r + \tfrac{1}{2}\sigma_r^2 r f_{rr}\}. \tag{54}$$

Equation (44) makes this drift $rF - C$. Therefore

$$\begin{aligned}\mathrm{d}F_t = {} & (r_t F_t - C_t)\,\mathrm{d}t + F_t\sigma_{C1}\sqrt{V_t}\,\mathrm{d}W_1^{\mathbb{Q}}(t) + F_t\sigma_{C2}\,\mathrm{d}W_2^{\mathbb{Q}}(t) \\ & + F_t\sigma_r\frac{f_r}{f}\sqrt{r_t}\,\mathrm{d}W_4^{\mathbb{Q}}(t).\end{aligned} \tag{55}$$

Returning to $\mathbb{P}$ adds $(\alpha^F)^\top\vartheta$ to the relative drift, where

$$\alpha^F = (\sigma_{C1}\sqrt{v}, \sigma_{C2}, \sigma_r(f_r/f)\sqrt{r})^\top. \tag{56}$$

To reproduce this vector with the risky assets, solve $L\pi^F = \alpha^F$. The W_2 row first gives

$$\sigma_{P2}\pi_I^F = \sigma_{C2} \quad \Longrightarrow \quad \pi_I^F = \frac{\sigma_{C2}}{\sigma_{P2}}. \tag{57}$$

The W_1 row then gives

$$\sqrt{v}(\pi_S^F + \sigma_{P1}\pi_I^F) = \sigma_{C1}\sqrt{v} \quad \Longrightarrow \quad \pi_S^F = \sigma_{C1} - \frac{\sigma_{P1}\sigma_{C2}}{\sigma_{P2}}. \tag{58}$$

Finally, the W_4 row gives

$$b_N\pi_N^F + b_I\pi_I^F = \sigma_r\frac{f_r}{f}, \tag{59}$$

which is the last formula in (47). This order of coefficient matching proves that the stock and indexed bond labels cannot be interchanged.

Step 2: Guarantee value. By (34), the terminal condition of the time t guarantee value is $G(T, p, r) = p\mathfrak{a}(r)$. Under $\mathbb{Q}$, the price level drift is η and the short-rate drift is $\kappa_r\theta_r - \bar{\kappa}_r r$. Because the candidate $G = pq(t, r)$ is linear in p and independent of v, the pp, pv, and all v derivatives in the full Feynman–Kac equation vanish. After division by p, the remaining pricing equation is exactly (46).

For $G(t, p, r) = pq(t, r)$, we have

$$G_p = q, \quad G_r = pq_r, \quad G_{pp} = G_{pr} = 0, \quad G_{rr} = pq_{rr}. \tag{60}$$

Under $\mathbb{Q}$, equation (14), Itô's formula, and (46) yield

$$\begin{aligned} \mathrm{d}G_t = {} & r_t G_t\,\mathrm{d}t + G_t\sigma_{P1}\sqrt{V_t}\,\mathrm{d}W_1^{\mathbb{Q}}(t) + G_t\sigma_{P2}\,\mathrm{d}W_2^{\mathbb{Q}}(t) \\ & + G_t\sigma_r\frac{q_r}{q}\sqrt{r_t}\,\mathrm{d}W_4^{\mathbb{Q}}(t). \end{aligned} \tag{61}$$

Thus

$$\alpha^G = (\sigma_{P1}\sqrt{v}, \sigma_{P2}, \sigma_r(q_r/q)\sqrt{r})^\top. \tag{62}$$

The coefficient equations for $L\pi^G = \alpha^G$ are

$$\sigma_{P2}\pi_I^G = \sigma_{P2}, \tag{63}$$

$$\sqrt{v}(\pi_S^G + \sigma_{P1}\pi_I^G) = \sigma_{P1}\sqrt{v}, \tag{64}$$

$$b_N\pi_N^G + b_I\pi_I^G = \sigma_r\frac{q_r}{q}. \tag{65}$$

They give $\pi_I^G = 1$, $\pi_S^G = 0$, and the nominal bond fraction in (48). Returning to $\mathbb{P}$ establishes (50).

Step 3: Self-financing auxiliary wealth. Write the pension equation in exposure form as follows:

$$\mathrm{d}X_t = [r_t X_t + (X_t L_t\pi_t)^\top\vartheta_t + C_t]\,\mathrm{d}t + (X_t L_t\pi_t)^\top\,\mathrm{d}W_t. \tag{66}$$

Add (49) and subtract (50). The contribution terms cancel and $rX + rF - rG = rY$. Hence

$$\mathrm{d}Y_t = [r_t Y_t + Y_t\alpha_t^\top\vartheta_t]\,\mathrm{d}t + Y_t\alpha_t^\top\,\mathrm{d}W_t, \tag{67}$$

where

$$Y_t\alpha_t = X_t L_t\pi_t + F_t\alpha_t^F - G_t\alpha_t^G. \tag{68}$$

Multiplication by L_t^{-1} proves (78).

Step 4: Real deflation. Let $a_P = \eta + \sigma_P(v)^\top \vartheta(v, r)$. From (8), we have

$$\frac{\mathrm{d}(P_t^{-1})}{P_t^{-1}} = [-a_P + |\sigma_P|^2]\,\mathrm{d}t - \sigma_P^\top\,\mathrm{d}W_t. \tag{69}$$

Using $Z = YP^{-1}$ and $\mathrm{d}\langle Y, P^{-1}\rangle/(YP^{-1}) = -\alpha^\top\sigma_P\,\mathrm{d}t$, we have

$$\frac{\mathrm{d}Z}{Z} = [r + \alpha^\top\vartheta - a_P + |\sigma_P|^2 - \alpha^\top\sigma_P]\,\mathrm{d}t + (\alpha - \sigma_P)^\top\,\mathrm{d}W. \tag{70}$$

Set $\beta = \alpha - \sigma_P$. Since $a_P = \eta + \sigma_P^\top\vartheta$,

$$\alpha^\top\vartheta - a_P + |\sigma_P|^2 - \alpha^\top\sigma_P = (\beta + \sigma_P)^\top\vartheta - \eta - \sigma_P^\top\vartheta + |\sigma_P|^2 - (\beta + \sigma_P)^\top\sigma_P \tag{71}$$

$$= -\eta + \beta^\top(\vartheta - \sigma_P). \tag{72}$$

Because $\vartheta - \sigma_P = \theta$, equation (81) follows. This completes the proof.

Remark 1. *Proposition 1, equation (17), of Wang and Jia [29] displays*

$$\pi_I^F = \frac{\sigma_{C1}\sigma_{P2} - \sigma_{C2}\sigma_{P1}}{\sigma_S\sigma_{P2}}, \qquad \pi_S^F = \frac{\sigma_{C2}}{\sigma_{P2}}. \tag{73}$$

The independent inflation shock is carried only by the indexed bond, so its coefficient equation is $\pi_I^F\sigma_{P2} = \sigma_{C2}$. Therefore, the stock and inflation indexed bond labels in (73) *are interchanged. In the constant volatility notation of that paper, coefficient matching gives*

$$\pi_I^F = \frac{\sigma_{C2}}{\sigma_{P2}}, \qquad \pi_S^F = \frac{\sigma_{C1}\sigma_{P2} - \sigma_{C2}\sigma_{P1}}{\sigma_S\sigma_{P2}}. \tag{74}$$

Equation (47) *is the Heston-scaled counterpart, with unit stock loading after the common $\sqrt{V_t}$ factor is removed. The proof of Proposition 2 shows the complete coefficient matching in the order W_2, W_1, and W_4.*

Define nominal auxiliary wealth and its real counterpart by

$$Y_t = X_t + F(t, T) - G(t), \qquad Z_t = \frac{Y_t}{P_t}. \tag{75}$$

Because $F(T, T) = 0$ and $G(T) = G_T$, we have

$$Z_T = \frac{X_T - G_T}{P_T}. \tag{76}$$

Let $\phi = (\phi_S, \phi_N, \phi_I)^\top$ be the risky asset fractions of Y. Adding (38) and (49) and subtracting (50) gives

$$\frac{\mathrm{d}Y_t}{Y_t} = [r_t + \alpha_t^\top\vartheta_t]\,\mathrm{d}t + \alpha_t^\top\,\mathrm{d}W_t, \qquad \alpha_t = L(t, V_t, r_t)\phi_t, \tag{77}$$

and the dollar holdings satisfy

$$Y_t\phi_t = X_t\pi_t + F_t\pi_t^F - G_t\pi_t^G. \tag{78}$$

Set

$$\sigma_P(v) = (\sigma_{P1}\sqrt{v}, \sigma_{P2}, 0)^\top, \qquad \beta = \alpha - \sigma_P(v), \tag{79}$$

$$\theta(v,r) = ((\lambda_S - \sigma_{P1})\sqrt{v}, \lambda_p - \sigma_{P2}, \lambda_r\sqrt{r})^\top. \tag{80}$$

Itô's formula gives the real self-financing equation

$$\frac{\mathrm{d}Z_t}{Z_t} = [r_t - \eta + \beta_t^\top \theta(V_t, r_t)]\,\mathrm{d}t + \beta_t^\top\,\mathrm{d}W_t. \tag{81}$$

The physical drift compensators in (8) cancel exactly in this deflation step.

The original problem is therefore equivalent to

$$\sup_{\beta\in\mathcal{A}} J^\beta(t,z,v,r), \qquad J^\beta = \int (u^\gamma)^{-1}\left(\mathbb{E}_{t,z,v,r}[u^\gamma(Z_T^\beta)]\right)\mathrm{d}\Gamma(\gamma), \tag{82}$$

subject to (81), (3), and (4). For a known original state, we have

$$V_1(t,x,p,c,v,r) = V(t,z,v,r), \qquad z = \frac{x + cf(t,r) - pq(t,r)}{p}. \tag{83}$$

Definition 2. *For an admissible candidate β^*, an alternative $\bar\beta$, and $h > 0$, let $\beta^h = \bar\beta$ on $[t, t+h)$ and $\beta^h = \beta^*$ afterward. The candidate is an equilibrium if*

$$\liminf_{h\downarrow 0} \frac{J^{\beta^*}(t,z,v,r) - J^{\beta^h}(t,z,v,r)}{h} \geq 0 \tag{84}$$

for every admissible local deviation. Its equilibrium value is $V = J^{\beta^*}$.

3.2. Verification theorem

For a smooth function $\Psi(t,z,v,r)$, define the spatial generator

$$\begin{aligned}\mathcal{A}^\beta\Psi = {} & z[r - \eta + \beta^\top\theta]\Psi_z + \kappa_v(\theta_v - v)\Psi_v + \kappa_r(\theta_r - r)\Psi_r \\ & + \tfrac{1}{2}z^2|\beta|^2\Psi_{zz} + \tfrac{1}{2}\sigma_v^2 v\Psi_{vv} + \tfrac{1}{2}\sigma_r^2 r\Psi_{rr} \\ & + \chi\sigma_v\sigma_r\sqrt{vr}\,\Psi_{vr} + z\sigma_v\sqrt{v}\,(\rho\beta_S + \chi\beta_r)\Psi_{zv} \\ & + z\sigma_r\sqrt{r}\,\beta_r\Psi_{zr}.\end{aligned} \tag{85}$$

Here $\beta = (\beta_S, \beta_P, \beta_r)^\top$ is ordered by (W_1, W_2, W_4). Define

$$\iota^\gamma(x) = \frac{\mathrm{d}}{\mathrm{d}x}(u^\gamma)^{-1}(x). \tag{86}$$

For an admissible β, let $L^2(Z^\beta, V, r)$ contain functions whose Itô martingale coefficient is square-integrable. Explicitly, for $h = h(t,z,v,r)$ this coefficient is

$$\Xi_h^\beta = (zh_z\beta_S + h_v\rho\sigma_v\sqrt{v}, zh_z\beta_P, zh_z\beta_r + h_v\chi\sigma_v\sqrt{v} + h_r\sigma_r\sqrt{r}, h_v\sigma_v\sqrt{v(1-\rho^2-\chi^2)}), \tag{87}$$

and the requirement is $\mathbb{E}[\int_t^T |\Xi_h^\beta|^2\,\mathrm{d}s] < \infty$.

Theorem 1. *Suppose that $U, Z^\gamma \in C^{1,2,2,2}([0,T]\times\mathbb{R}^3_+)$ for every γ in the support of Γ, and put*

$$H(t,z,v,r) = \int (u^\gamma)^{-1}(Z^\gamma(t,z,v,r))\,\mathrm{d}\Gamma(\gamma). \tag{88}$$

Assume

$$U_t = \inf_\beta \Big\{ -\mathcal{A}^\beta U + H_t + \mathcal{A}^\beta H - \int \iota^\gamma(Z^\gamma)[Z^\gamma_t + \mathcal{A}^\beta Z^\gamma]\,\mathrm{d}\Gamma(\gamma)\Big\}, \tag{89}$$

$$Z^\gamma_t = -\mathcal{A}^{\beta^*} Z^\gamma, \tag{90}$$

where β^* attains the infimum, with terminal conditions

$$U(T,z,v,r) = z, \qquad Z^\gamma(T,z,v,r) = u^\gamma(z). \tag{91}$$

Assume also that $U, H, Z^\gamma \in L^2(Z^{\beta^*}, V, r)$, that the needed family is uniformly integrable in γ, and that β^* is admissible. Then β^* is an equilibrium and

$$V = U = H, \qquad Z^\gamma(t,z,v,r) = \mathbb{E}_{t,z,v,r}[u^\gamma(Z^{\beta^*}_T)]. \tag{92}$$

Proof. For compactness write $\xi = (z,v,r)$ and $K_\gamma = (u^\gamma)^{-1}$. The regularity assumptions and Feynman–Kac formula applied to (90) give

$$Z^\gamma(t,\xi) = \mathbb{E}_{t,\xi}[u^\gamma(Z^{\beta^*}_T)] \tag{93}$$

for every γ.

Set $\beta = \beta^*$ in (89). Equation (90) removes the integral term, so

$$U_t = -\mathcal{A}^{\beta^*} U + H_t + \mathcal{A}^{\beta^*} H. \tag{94}$$

Itô's formula, localization, and the L^2 assumptions imply

$$\mathbb{E}_{t,\xi}[U(T,\xi^{\beta^*}_T)] = U(t,\xi) + \mathbb{E}_{t,\xi}\int_t^T (U_s + \mathcal{A}^{\beta^*} U)(s,\xi_s)\,\mathrm{d}s, \tag{95}$$

$$\mathbb{E}_{t,\xi}[H(T,\xi^{\beta^*}_T)] = H(t,\xi) + \mathbb{E}_{t,\xi}\int_t^T (H_s + \mathcal{A}^{\beta^*} H)(s,\xi_s)\,\mathrm{d}s. \tag{96}$$

The terminal conditions give $U(T,\xi) = H(T,\xi) = z$. Subtracting (96) from (95) and using (94) yields $U = H$. With (93), we have

$$U = H = \int K_\gamma(Z^\gamma)\,\mathrm{d}\Gamma(\gamma) = \int K_\gamma(\mathbb{E}_t[u^\gamma(Z^{\beta^*}_T)])\,\mathrm{d}\Gamma(\gamma) = J^{\beta^*}. \tag{97}$$

We next prove the local deviation condition. Fix $\bar\beta$ on $[t,t+h)$ and use β^* afterward. By the Markov property, we have

$$\mathbb{E}_{t,\xi}[u^\gamma(Z^{\beta^h}_T)] = \mathbb{E}_{t,\xi}[Z^\gamma(t+h,\xi^{\beta^h}_{t+h})]. \tag{98}$$

Apply Itô's formula over $[t,t+h]$. Uniform integrability makes the martingale expectation zero and continuity gives

$$\mathbb{E}_{t,\xi}[u^\gamma(Z^{\beta^h}_T)] = Z^\gamma(t,\xi) + h[Z^\gamma_t + \mathcal{A}^{\bar\beta} Z^\gamma](t,\xi) + o(h), \tag{99}$$

where the remainder is uniform in γ on its compact support. Taylor expansion of K_γ around $Z^\gamma(t,\xi)$ gives

$$K_\gamma(\mathbb{E}_t[u^\gamma(Z_T^{\beta^h})]) - K_\gamma(Z^\gamma) = h\iota^\gamma(Z^\gamma)[Z_t^\gamma + \mathcal{A}^{\bar\beta} Z^\gamma] + o(h). \tag{100}$$

Dominated convergence permits integration over Γ.

Since $U = H$, equation (89) becomes

$$0 = \inf_\beta \left\{ - \int \iota^\gamma(Z^\gamma)[Z_t^\gamma + \mathcal{A}^\beta Z^\gamma]\, \mathrm{d}\Gamma(\gamma) \right\}. \tag{101}$$

Equivalently, β^* maximizes the integral and its value is zero because (90) holds. Thus, for every $\bar\beta$, we have

$$\int \iota^\gamma(Z^\gamma)[Z_t^\gamma + \mathcal{A}^{\bar\beta} Z^\gamma]\, \mathrm{d}\Gamma(\gamma) \le 0. \tag{102}$$

Equations (100) and (102) imply

$$J^{\beta^h}(t,\xi) - J^{\beta^*}(t,\xi) \le o(h), \tag{103}$$

which is exactly (84) after division by h and passage to the lower limit.

It remains to calculate the maximizer. All control-dependent terms in the integrated Hamiltonian are

$$\mathcal{H}(\beta) = \mathcal{H}_0 + z\mathcal{M}_z \beta^\top \theta + \tfrac{1}{2} z^2 \mathcal{M}_{zz} |\beta|^2 + z\sigma_v \sqrt{v}\, \mathcal{M}_{zv}(\rho\beta_S + \chi\beta_r) + z\sigma_r \sqrt{r}\, \mathcal{M}_{zr}\beta_r. \tag{104}$$

Therefore

$$\partial_{\beta_S}\mathcal{H} = z\mathcal{M}_z(\lambda_S - \sigma_{P1})\sqrt{v} + z^2\mathcal{M}_{zz}\beta_S + z\rho\sigma_v\sqrt{v}\mathcal{M}_{zv}, \tag{105}$$

$$\partial_{\beta_P}\mathcal{H} = z\mathcal{M}_z(\lambda_p - \sigma_{P2}) + z^2\mathcal{M}_{zz}\beta_P, \tag{106}$$

$$\partial_{\beta_r}\mathcal{H} = z\mathcal{M}_z\lambda_r\sqrt{r} + z^2\mathcal{M}_{zz}\beta_r + z\chi\sigma_v\sqrt{v}\mathcal{M}_{zv} + z\sigma_r\sqrt{r}\mathcal{M}_{zr}. \tag{107}$$

The Hessian is $z^2\mathcal{M}_{zz}I_3$. It is negative definite when $\mathcal{M}_{zz} < 0$, so setting the gradient to zero gives the unique formulas (117)–(119).

Remark 2. *Theorem 1 verifies the equilibrium feedback under a sufficiently regular solution, admissible feedback, square integrability, and uniform integrability. Lemma 1 establishes the local classical existence and a continuation criterion for a finite two-point distribution on a stopped positive state rectangle. For a general distribution* Γ*, the system characterizes and conditionally verifies an equilibrium candidate. The associated aggregate feedback fixed-point construction is stated after the power utility reduction.*

We now perform the chain rule reduction explicitly. Write $K_\gamma = (u^\gamma)^{-1}$ and, for $i, j \in \{z, v, r\}$, define

$$\begin{aligned}
\mathcal{M}_z &= \int \iota^\gamma(Z^\gamma) Z_z^\gamma\, \mathrm{d}\Gamma, & \mathcal{M}_{zz} &= \int \iota^\gamma(Z^\gamma) Z_{zz}^\gamma\, \mathrm{d}\Gamma, \\
\mathcal{M}_{zv} &= \int \iota^\gamma(Z^\gamma) Z_{zv}^\gamma\, \mathrm{d}\Gamma, & \mathcal{M}_{zr} &= \int \iota^\gamma(Z^\gamma) Z_{zr}^\gamma\, \mathrm{d}\Gamma, \\
\mathcal{M}_i &= \int \iota^\gamma(Z^\gamma) Z_i^\gamma\, \mathrm{d}\Gamma, & \mathcal{M}_{ij} &= \int \iota^\gamma(Z^\gamma) Z_{ij}^\gamma\, \mathrm{d}\Gamma,
\end{aligned} \tag{108}$$

$$\mathcal{R}_{ij} = \int (\iota^\gamma)'(Z^\gamma) Z_i^\gamma Z_j^\gamma\, \mathrm{d}\Gamma. \tag{109}$$

The first and second derivatives of H are

$$H_t = \int \iota^\gamma(Z^\gamma) Z_t^\gamma \, \mathrm{d}\Gamma, \qquad H_i = \mathcal{M}_i, \tag{110}$$

$$H_{ij} = \mathcal{M}_{ij} + \mathcal{R}_{ij}, \qquad i, j \in \{z, v, r\}. \tag{111}$$

Thus every time and first-order term in $H_t + \mathcal{A}^\beta H - \int \iota^\gamma(Z^\gamma)[Z_t^\gamma + \mathcal{A}^\beta Z^\gamma] \, \mathrm{d}\Gamma$ cancels. Only the chain rule remainders from the diffusion terms remain, and (89) becomes

$$\begin{aligned} U_t = \inf_\beta \Big\{ & - \mathcal{A}^\beta U + \tfrac{1}{2} z^2 |\beta|^2 \mathcal{R}_{zz} + \tfrac{1}{2} \sigma_v^2 v \mathcal{R}_{vv} + \tfrac{1}{2} \sigma_r^2 r \mathcal{R}_{rr} \\ & + \chi \sigma_v \sigma_r \sqrt{vr} \, \mathcal{R}_{vr} + z \sigma_v \sqrt{v} \, (\rho \beta_S + \chi \beta_r) \mathcal{R}_{zv} + z \sigma_r \sqrt{r} \, \beta_r \mathcal{R}_{zr} \Big\}. \end{aligned} \tag{112}$$

The verification identity $U = H$ then gives $U_i = \mathcal{M}_i$ and $U_{ij} = \mathcal{M}_{ij} + \mathcal{R}_{ij}$. Substituting these identities into (112) cancels every $\mathcal{R}$ term involving the control. Equivalently, the minimizing control maximizes the quadratic

$$\mathcal{H}(\beta) = z \mathcal{M}_z \beta^\top \theta + \tfrac{1}{2} z^2 \mathcal{M}_{zz} |\beta|^2 + z \sigma_v \sqrt{v} \, \mathcal{M}_{zv} (\rho \beta_S + \chi \beta_r) + z \sigma_r \sqrt{r} \, \mathcal{M}_{zr} \beta_r. \tag{113}$$

Its three first-order conditions are

$$0 = z(\lambda_S - \sigma_{P1}) \sqrt{v} \, \mathcal{M}_z + z^2 \mathcal{M}_{zz} \beta_S + z \rho \sigma_v \sqrt{v} \, \mathcal{M}_{zv}, \tag{114}$$

$$0 = z(\lambda_p - \sigma_{P2}) \mathcal{M}_z + z^2 \mathcal{M}_{zz} \beta_P, \tag{115}$$

$$0 = z \lambda_r \sqrt{r} \, \mathcal{M}_z + z^2 \mathcal{M}_{zz} \beta_r + z \chi \sigma_v \sqrt{v} \, \mathcal{M}_{zv} + z \sigma_r \sqrt{r} \, \mathcal{M}_{zr}. \tag{116}$$

The Hessian of $\mathcal{H}$ is $z^2 \mathcal{M}_{zz} I_3$. Hence, if $\mathcal{M}_{zz} < 0$, the quadratic is strictly concave and the first-order conditions are sufficient. Solving them gives

$$\beta_S^* = - \frac{(\lambda_S - \sigma_{P1}) \sqrt{v} \, \mathcal{M}_z + \rho \sigma_v \sqrt{v} \, \mathcal{M}_{zv}}{z \mathcal{M}_{zz}}, \tag{117}$$

$$\beta_P^* = - \frac{(\lambda_p - \sigma_{P2}) \mathcal{M}_z}{z \mathcal{M}_{zz}}, \tag{118}$$

$$\beta_r^* = - \frac{\lambda_r \sqrt{r} \, \mathcal{M}_z + \chi \sigma_v \sqrt{v} \, \mathcal{M}_{zv} + \sigma_r \sqrt{r} \, \mathcal{M}_{zr}}{z \mathcal{M}_{zz}}. \tag{119}$$

The proof of Theorem 1 derives the same identities from the spike deviation expansion and verifies that the stationary point is the unique optimizer.

4. Equilibrium investment strategies

4.1. Power utility reduction

For the power utility in (39), we have

$$(u^\gamma)^{-1}(x) = \{(1 - \gamma) x\}^{1/(1-\gamma)}, \qquad \iota^\gamma(x) = \{(1 - \gamma) x\}^{\gamma/(1-\gamma)}. \tag{120}$$

Following the benchmark derivation, posit

$$Z^\gamma(t,z,v,r) = \frac{1}{1-\gamma}[g^\gamma(t,v,r)]^\gamma z^{1-\gamma}, \qquad g^\gamma(T,v,r) = 1. \tag{121}$$

We require $g^\gamma > 0$. Define

$$w^\gamma = (g^\gamma)^{\gamma/(1-\gamma)}, \qquad M_0 = \int w^\gamma \, \mathrm{d}\Gamma(\gamma), \qquad M_1 = \int \gamma w^\gamma \, \mathrm{d}\Gamma(\gamma), \tag{122}$$

$$M_v = \int \gamma w^\gamma \frac{g_v^\gamma}{g^\gamma} \, \mathrm{d}\Gamma(\gamma), \qquad M_r = \int \gamma w^\gamma \frac{g_r^\gamma}{g^\gamma} \, \mathrm{d}\Gamma(\gamma), \qquad \varepsilon(t,v,r;\Gamma) = \frac{M_1}{M_0}. \tag{123}$$

The quantity ε is the state-dependent effective risk aversion. For positive weights, it lies between the smallest and largest values in the support of Γ.

Theorem 2. *Suppose the system below has a positive classical solution satisfying the hypotheses of Theorem 1. Then the formulas below conditionally verify an equilibrium feedback. For a general distribution Γ, this verification is conditional on the existence of such a solution and on satisfaction of the aggregate feedback fixed-point condition. The equilibrium real wealth exposures are*

$$\beta_S^* = \sqrt{v}\,\frac{(\lambda_S - \sigma_{P1})M_0 + \rho\sigma_v M_v}{M_1}, \tag{124}$$

$$\beta_P^* = (\lambda_p - \sigma_{P2})\frac{M_0}{M_1}, \tag{125}$$

$$\beta_r^* = \frac{\lambda_r \sqrt{r}\, M_0 + \chi\sigma_v \sqrt{v}\, M_v + \sigma_r \sqrt{r}\, M_r}{M_1}. \tag{126}$$

For every γ in the support of Γ, g^γ solves

$$\begin{aligned} 0 = {} & g_t^\gamma + \kappa_v(\theta_v - v)g_v^\gamma + \tfrac{1}{2}\sigma_v^2 v\left[g_{vv}^\gamma + (\gamma-1)\frac{(g_v^\gamma)^2}{g^\gamma}\right] \\ & + \kappa_r(\theta_r - r)g_r^\gamma + \tfrac{1}{2}\sigma_r^2 r\left[g_{rr}^\gamma + (\gamma-1)\frac{(g_r^\gamma)^2}{g^\gamma}\right] \\ & + \chi\sigma_v\sigma_r\sqrt{vr}\left[g_{vr}^\gamma + (\gamma-1)\frac{g_v^\gamma g_r^\gamma}{g^\gamma}\right] \\ & + \frac{1-\gamma}{\gamma}\left[r - \eta + (\beta^*)^\top\theta(v,r) - \frac{\gamma}{2}|\beta^*|^2\right]g^\gamma \\ & + (1-\gamma)\sigma_v\sqrt{v}\,(\rho\beta_S^* + \chi\beta_r^*)g_v^\gamma + (1-\gamma)\sigma_r\sqrt{r}\,\beta_r^* g_r^\gamma, \qquad g^\gamma(T,v,r) = 1. \end{aligned} \tag{127}$$

The corresponding auxiliary wealth asset fractions are

$$\phi_I^* = 1 + \left(\frac{\lambda_p}{\sigma_{P2}} - 1\right)\frac{1}{\varepsilon}, \tag{128}$$

$$\phi_S^* = \left(\lambda_S - \frac{\lambda_p\sigma_{P1}}{\sigma_{P2}}\right)\frac{1}{\varepsilon} + \rho\sigma_v\frac{M_v}{M_1}, \tag{129}$$

$$\phi_N^* = \frac{\lambda_r/\varepsilon + \chi\sigma_v\sqrt{v/r}\,M_v/M_1 + \sigma_r M_r/M_1 - b_I\phi_I^*}{b_N}. \tag{130}$$

Finally, we have

$$U(t,z,v,r) = H(t,z,v,r) = z\int w^\gamma(t,v,r)\,\mathrm{d}\Gamma(\gamma). \tag{131}$$

Proof. For the ansatz (121), direct differentiation gives

$$\begin{aligned} Z^\gamma_z &= (g^\gamma)^\gamma z^{-\gamma}, & Z^\gamma_{zz} &= -\gamma(g^\gamma)^\gamma z^{-\gamma-1}, \\ Z^\gamma_{zv} &= \gamma(g^\gamma)^{\gamma-1} g^\gamma_v z^{-\gamma}, & Z^\gamma_{zr} &= \gamma(g^\gamma)^{\gamma-1} g^\gamma_r z^{-\gamma}. \end{aligned} \tag{132}$$

Moreover, we have

$$\begin{aligned} \frac{Z^\gamma_t}{Z^\gamma} &= \gamma\frac{g^\gamma_t}{g^\gamma}, & \frac{Z^\gamma_v}{Z^\gamma} &= \gamma\frac{g^\gamma_v}{g^\gamma}, & \frac{Z^\gamma_r}{Z^\gamma} &= \gamma\frac{g^\gamma_r}{g^\gamma}, \\ \frac{Z^\gamma_{vv}}{Z^\gamma} &= \gamma\frac{g^\gamma_{vv}}{g^\gamma} + \gamma(\gamma-1)\left(\frac{g^\gamma_v}{g^\gamma}\right)^2, & \frac{Z^\gamma_{rr}}{Z^\gamma} &= \gamma\frac{g^\gamma_{rr}}{g^\gamma} + \gamma(\gamma-1)\left(\frac{g^\gamma_r}{g^\gamma}\right)^2, \\ \frac{Z^\gamma_{vr}}{Z^\gamma} &= \gamma\frac{g^\gamma_{vr}}{g^\gamma} + \gamma(\gamma-1)\frac{g^\gamma_v g^\gamma_r}{(g^\gamma)^2}. \end{aligned} \tag{133}$$

At Z^γ, equation (120) gives

$$\iota^\gamma(Z^\gamma) = (g^\gamma)^{\gamma^2/(1-\gamma)} z^\gamma. \tag{134}$$

Multiplication by (132) yields

$$\begin{aligned} \iota^\gamma Z^\gamma_z &= w^\gamma, & \iota^\gamma Z^\gamma_{zz} &= -\frac{\gamma}{z}w^\gamma, \\ \iota^\gamma Z^\gamma_{zv} &= \gamma w^\gamma\frac{g^\gamma_v}{g^\gamma}, & \iota^\gamma Z^\gamma_{zr} &= \gamma w^\gamma\frac{g^\gamma_r}{g^\gamma}. \end{aligned} \tag{135}$$

Consequently, we have

$$\mathcal{M}_z = M_0, \qquad \mathcal{M}_{zz} = -M_1/z, \qquad \mathcal{M}_{zv} = M_v, \qquad \mathcal{M}_{zr} = M_r. \tag{136}$$

Because $w^\gamma > 0$ and $\gamma > 0$, $M_1 > 0$ and $\mathcal{M}_{zz} < 0$. Substitution in (117)–(119) proves (124)–(126).

Next substitute (132)–(133) into $Z^\gamma_t + \mathcal{A}^{\beta^*} Z^\gamma = 0$. Division by Z^γ gives

$$\begin{aligned} 0 = {} & \gamma\frac{g^\gamma_t}{g^\gamma} + \gamma\kappa_v(\theta_v - v)\frac{g^\gamma_v}{g^\gamma} + \frac{\sigma_v^2 v}{2}\left[\gamma\frac{g^\gamma_{vv}}{g^\gamma} + \gamma(\gamma-1)\left(\frac{g^\gamma_v}{g^\gamma}\right)^2\right] \\ & + \gamma\kappa_r(\theta_r - r)\frac{g^\gamma_r}{g^\gamma} + \frac{\sigma_r^2 r}{2}\left[\gamma\frac{g^\gamma_{rr}}{g^\gamma} + \gamma(\gamma-1)\left(\frac{g^\gamma_r}{g^\gamma}\right)^2\right] \\ & + \chi\sigma_v\sigma_r\sqrt{vr}\left[\gamma\frac{g^\gamma_{vr}}{g^\gamma} + \gamma(\gamma-1)\frac{g^\gamma_v g^\gamma_r}{(g^\gamma)^2}\right] \\ & + (1-\gamma)\left[r - \eta + (\beta^*)^\top\theta(v,r)\right] - \frac{\gamma(1-\gamma)}{2}|\beta^*|^2 \\ & + \gamma(1-\gamma)\sigma_v\sqrt{v}\,(\rho\beta^*_S + \chi\beta^*_r)\frac{g^\gamma_v}{g^\gamma} + \gamma(1-\gamma)\sigma_r\sqrt{r}\,\beta^*_r\frac{g^\gamma_r}{g^\gamma}. \end{aligned} \tag{137}$$

The wealth derivative ratios used in the last two lines are

$$\frac{zZ_z^\gamma}{Z^\gamma} = 1-\gamma, \qquad \frac{z^2 Z_{zz}^\gamma}{Z^\gamma} = -\gamma(1-\gamma), \tag{138}$$

while

$$\frac{zZ_{zv}^\gamma}{Z^\gamma} = \gamma(1-\gamma)\frac{g_v^\gamma}{g^\gamma}, \qquad \frac{zZ_{zr}^\gamma}{Z^\gamma} = \gamma(1-\gamma)\frac{g_r^\gamma}{g^\gamma}. \tag{139}$$

Multiplying (137) by g^γ/γ produces every term in (127), including the mixed state derivative and the two wealth–state hedge terms. The terminal identity $Z^\gamma(T,z,v,r) = u^\gamma(z)$ gives $[g^\gamma(T,v,r)]^\gamma = 1$; positivity of g^γ therefore forces $g^\gamma(T,v,r) = 1$.

Finally solve $L\phi = \alpha = \beta + \sigma_P$. The W_2 row gives

$$\phi_I = \frac{\beta_P + \sigma_{P2}}{\sigma_{P2}} = 1 + \left(\frac{\lambda_p}{\sigma_{P2}} - 1\right)\frac{1}{\varepsilon}. \tag{140}$$

The W_1 row gives

$$\phi_S = \frac{\beta_S + \sigma_{P1}\sqrt{v} - \sigma_{P1}\sqrt{v}\,\phi_I}{\sqrt{v}} \tag{141}$$

$$= \left(\lambda_S - \frac{\lambda_p \sigma_{P1}}{\sigma_{P2}}\right)\frac{1}{\varepsilon} + \rho\sigma_v \frac{M_v}{M_1}. \tag{142}$$

The W_4 row gives

$$b_N\phi_N + b_I\phi_I = \frac{\beta_r}{\sqrt{r}}, \tag{143}$$

$$\phi_N = \frac{\beta_r/\sqrt{r} - b_I\phi_I}{b_N} = \frac{\lambda_r/\varepsilon + \chi\sigma_v\sqrt{v/r}\,M_v/M_1 + \sigma_r M_r/M_1 - b_I\phi_I}{b_N}, \tag{144}$$

which is (130). Moreover, we have

$$(u^\gamma)^{-1}(Z^\gamma) = z(g^\gamma)^{\gamma/(1-\gamma)} = zw^\gamma, \tag{145}$$

which proves (131). Reversing the calculations verifies the candidate system.

Remark 3. *For a general distribution* Γ*, let* β *be an admissible aggregate feedback, solve the family of equation* (127) *with* β *held fixed, and form* $M_0^\beta, M_1^\beta, M_v^\beta, M_r^\beta$ *from* (122)–(123)*. Substitution of these aggregates into* (124)–(126) *defines an aggregate control map* $\mathcal{T}(\beta)$*. A general distribution equilibrium must satisfy* $\beta = \mathcal{T}(\beta)$*. This is a fixed-point characterization; the local existence result in this paper is confined to the finite two-point system.*

Equations (128) and (129) have the same economic decomposition as the benchmark formulas. The terms proportional to $1/\varepsilon$ are myopic and inflation-hedging demands. The term $\rho\sigma_v M_v/M_1$ is the stock-side Heston variance hedge. Equation (130) now contains two continuation hedges: the CIR duration hedge $\sigma_r M_r/M_1$ and the cross-hedge $\chi\sigma_v\sqrt{v/r}\,M_v/M_1$. The latter is the implementable new channel: A nominal bond partly hedges variance continuation risk because the variance process loads on the traded rate shock. The indexed bond rate exposure is subtracted to obtain the nominal bond position. Setting $\chi = 0$ removes only the cross-hedge and recovers the independent factor Heston–CIR system. When also $\sigma_v = \sigma_r = 0$ and r is constant, the state gradients vanish and the benchmark ordinary differential equation (ODE) system and strategies are recovered after replacing $\sqrt{v}$ by the constant stock volatility.

4.2. Two-point and one-point distributions for risk aversion

Suppose

$$\mathbb{P}(\gamma = \gamma_1) = p_1, \qquad \mathbb{P}(\gamma = \gamma_2) = p_2, \qquad p_1 + p_2 = 1, \qquad 0 < \gamma_1 < \gamma_2, \qquad \gamma_i \neq 1. \tag{146}$$

Writing $g_i = g^{\gamma_i}$ and $w_i = g_i^{\gamma_i/(1-\gamma_i)}$, we obtain

$$\begin{aligned} M_0 &= p_1 w_1 + p_2 w_2, & M_1 &= p_1\gamma_1 w_1 + p_2\gamma_2 w_2, \\ M_v &= p_1\gamma_1 w_1 \frac{g_{1,v}}{g_1} + p_2\gamma_2 w_2 \frac{g_{2,v}}{g_2}, & M_r &= p_1\gamma_1 w_1 \frac{g_{1,r}}{g_1} + p_2\gamma_2 w_2 \frac{g_{2,r}}{g_2}, \end{aligned} \tag{147}$$

$$\varepsilon(t, v, r; \Gamma) = \frac{p_1\gamma_1 w_1 + p_2\gamma_2 w_2}{p_1 w_1 + p_2 w_2} \in [\gamma_1, \gamma_2]. \tag{148}$$

Equation (127) for γ_1 and γ_2, together with (147), form two coupled semilinear PDEs. This is the direct Heston–CIR counterpart of the benchmark's three-dimensional ODE representation.

Lemma 1. *Let $D = [\underline{v}, \bar{v}] \times [\underline{r}, \bar{r}]$ with $\underline{v}, \underline{r} > 0$, and impose positive $C^{2+\alpha}$ boundary data that are compatible with $g_i(T, \cdot) = 1$. Then the two-point terminal value system has a positive classical solution on $[T - \delta, T] \times D$ for some $\delta > 0$. The solution can be continued backward while its $C^{1,2,2}$ norm remains finite, and both $\min_i g_i$ and M_1 remain bounded away from zero.*

Proof. Set $\tau = T - t$. On D, the principal diffusion matrix is

$$\frac{1}{2}\begin{pmatrix} \sigma_v^2 v & \chi\sigma_v\sigma_r\sqrt{vr} \\ \chi\sigma_v\sigma_r\sqrt{vr} & \sigma_r^2 r \end{pmatrix}. \tag{149}$$

Its determinant is $\frac{1}{4}\sigma_v^2\sigma_r^2 vr(1 - \chi^2) > 0$ and its trace is positive. More precisely, if $A(v, r)$ denotes the matrix in (149), then

$$\begin{aligned} \lambda_{\min}(A(v, r)) &= \frac{\det A(v, r)}{\lambda_{\max}(A(v, r))} \geq \frac{\det A(v, r)}{\operatorname{tr} A(v, r)} \\ &\geq \frac{\sigma_v^2\sigma_r^2 \underline{v}\,\underline{r}(1 - \chi^2)}{2(\sigma_v^2\bar{v} + \sigma_r^2\bar{r})} =: a_D > 0. \end{aligned} \tag{150}$$

Thus the two-component system is uniformly parabolic on D. On the open set

$$\mathcal{O} = \{(g_1, g_2, \nabla g_1, \nabla g_2) : g_1 > 0, g_2 > 0, M_1 > 0\}, \tag{151}$$

the powers w_i, the ratios $g_{i,v}/g_i$ and $g_{i,r}/g_i$, the moments in (147), and the feedbacks in (124)–(126) are smooth functions of their arguments. Write the system obtained from (127) in forward time as

$$\partial_\tau g_i = \operatorname{tr}(AD^2 g_i) + \mathcal{F}_i(v, r, g_1, g_2, \nabla g_1, \nabla g_2), \qquad i = 1, 2. \tag{152}$$

Let $c_0 = p_1\gamma_1 + p_2\gamma_2$ and fix $0 < \varepsilon < \min\{1/2, c_0/2\}$. On the closed set

$$\mathcal{K}_\varepsilon = \{g_i \in [1/2, 3/2], \quad M_1 \in [c_0/2, 2c_0], \quad |\nabla g_i| \leq \varepsilon\} \subset \mathcal{O}, \tag{153}$$

there is a finite L_ε such that

$$|\mathcal{F}_i(v, r, q, p) - \mathcal{F}_i(v, r, \tilde{q}, \tilde{p})| \leq L_\varepsilon\left(|q - \tilde{q}| + |p - \tilde{p}|\right), \qquad (q, p), (\tilde{q}, \tilde{p}) \in \mathcal{K}_\varepsilon. \tag{154}$$

Indeed, all denominators in (147) and (124)–(126) are bounded below on $\mathcal{K}_\varepsilon$, so the derivatives of $\mathcal{F}_i$ are bounded there. The terminal datum $(g_1, g_2) = (1, 1)$ belongs to the interior of $\mathcal{K}_\varepsilon$ and has $M_1 = c_0$. Uniform parabolicity (150) and (154) yield a unique classical solution of (152) for $0 \le \tau \le \delta$ for some $\delta > 0$ [30]. Shrinking δ, if necessary, gives

$$\min_{i=1,2} \inf_{[0,\delta]\times D} g_i \ge \frac{1}{2}, \qquad \inf_{[0,\delta]\times D} M_1 \ge \frac{c_0}{2}. \tag{155}$$

If $\tau_0 < T$ is a backward continuation time at which the $C^{1,2,2}$ norm is finite and the two lower bounds in (155) hold with positive constants, the same construction with terminal data $g_i(T - \tau_0, \cdot)$ gives a further interval of existence. This proves the continuation criterion.

Moreover, we have

$$\gamma_1 \le \varepsilon = \frac{p_1\gamma_1 w_1 + p_2\gamma_2 w_2}{p_1 w_1 + p_2 w_2} \le \gamma_2 \tag{156}$$

whenever $g_i > 0$. Hence $M_1 = \varepsilon M_0$ remains bounded away from zero while the positive weights remain finite. The continuation condition additionally requires bounded spatial derivatives for the coupled PDE system.

The differentiation step used in the benchmark remains valid pointwise in (v, r). Define

$$s_i(t, v, r) = \frac{\gamma_i}{1 - \gamma_i} \frac{g_{i,t}}{g_i}. \tag{157}$$

Then

$$\varepsilon_t = \frac{p_1 p_2 w_1 w_2 (\gamma_1 - \gamma_2)(s_1 - s_2)}{(p_1 w_1 + p_2 w_2)^2}. \tag{158}$$

In the present state-dependent setting, s_i contains the spatial derivatives in (127); consequently, (158) forms part of the coupled PDE system.

Proposition 3. *Fix compact state bounds $0 < \underline{v} < \bar{v}$ and $0 < \underline{r} < \bar{r}$. Suppose that the two-point system has positive solutions $g_i \in C^{1,2,2}$ on the resulting cylinder, g_i, g_i^{-1}, and their first state derivatives are bounded, and the boundary conditions are compatible with the stopped Heston–CIR process. Then the candidate functions in Theorem 2 satisfy Theorem 1 up to the exit time. If the same bounds are replaced by the polynomial growth and uniform integrability conditions stated in the proof below, the conclusion holds on the full state space.*

Proof. On the stopped state cylinder, fix constants $0 < m_g \le M_g < \infty$ and $M_\nabla < \infty$ such that

$$m_g \le g_i \le M_g, \qquad |g_{i,v}| + |g_{i,r}| \le M_\nabla, \qquad i = 1, 2. \tag{159}$$

For $a_i = \gamma_i/(1 - \gamma_i)$, set

$$\underline{w} = \min_{i=1,2} \min\{m_g^{a_i}, M_g^{a_i}\}, \qquad \overline{w} = \max_{i=1,2} \max\{m_g^{a_i}, M_g^{a_i}\}. \tag{160}$$

Then $0 < \underline{w} \le w_i \le \overline{w}$, and hence

$$\gamma_1 \underline{w} \le M_1 = p_1\gamma_1 w_1 + p_2\gamma_2 w_2 \le \gamma_2 \overline{w}. \tag{161}$$

Equation (148) then gives

$$0 < \gamma_1 \le \varepsilon(t, v, r; \Gamma) \le \gamma_2. \tag{162}$$

Moreover,

$$\left|\frac{M_v}{M_1}\right| + \left|\frac{M_r}{M_1}\right| \le \frac{2\gamma_2 \overline{w} M_\nabla}{\gamma_1 \underline{w}\, m_g} =: C_M. \tag{163}$$

Since v and r are bounded on the cylinder, (124)–(126) yield a constant $C_\beta < \infty$ satisfying

$$\sup_{[t,T\wedge\tau]} |\beta_s^*| \le C_\beta. \tag{164}$$

The controlled real wealth is geometric.

$$\frac{\mathrm{d}Z_t}{Z_t} = [r_t - \eta + (\beta_t^*)^\top \theta_t]\,\mathrm{d}t + (\beta_t^*)^\top \,\mathrm{d}W_t. \tag{165}$$

Writing $b_s = r_s - \eta + (\beta_s^*)^\top \theta_s$, the explicit solution is

$$Z_s = z \exp\left\{\int_t^s \left(b_u - \frac{1}{2}|\beta_u^*|^2\right)\mathrm{d}u + \int_t^s (\beta_u^*)^\top \,\mathrm{d}W_u\right\}. \tag{166}$$

The stopped coefficients b and β^* are bounded. Therefore, for every $q \in \mathbb{R}$, the exponential martingale identity gives

$$\mathbb{E}_{t,z,v,r}\left[\sup_{t\le s\le T\wedge\tau} Z_s^q\right] \le z^q \exp\{C_q(T-t)\}\mathbb{E}_{t,z,v,r}\left[\sup_{t\le s\le T\wedge\tau} \mathcal{E}\left(q\int_t^s (\beta_u^*)^\top \,\mathrm{d}W_u\right)\right] < \infty, \tag{167}$$

where C_q depends only on q, the stopped cylinder, and C_β. In particular, for $i = 1, 2$,

$$\mathbb{E}_{t,z,v,r}\int_t^{T\wedge\tau} \left(Z_s^{1-\gamma_i} + Z_s\right)^2 \mathrm{d}s < \infty. \tag{168}$$

The derivatives of

$$Z^{\gamma_i}(t,z,v,r) = \frac{1}{1-\gamma_i} g_i(t,v,r)^{\gamma_i} z^{1-\gamma_i} \tag{169}$$

are products of $z^{1-\gamma_i}$ with bounded functions and bounded first derivatives. Consequently, there is a constant C_i such that

$$\left|\Xi^{\beta^*}_{Z^{\gamma_i}}(s, Z_s, V_s, r_s)\right| \le C_i\left(Z_s^{1-\gamma_i} + Z_s\right), \qquad s \le T \wedge \tau. \tag{170}$$

Equations (170) and (168) give

$$\mathbb{E}_{t,z,v,r}\int_t^{T\wedge\tau} \left|\Xi^{\beta^*}_{Z^{\gamma_i}}\right|^2 \mathrm{d}s < \infty, \qquad i = 1, 2. \tag{171}$$

Thus $Z^{\gamma_i} \in L^2$. Further, we have

$$U = H = z[p_1 w_1 + p_2 w_2]. \tag{172}$$

Its first derivatives are products of z with bounded functions, and hence

$$\left|\Xi^{\beta^*}_U\right| + \left|\Xi^{\beta^*}_H\right| \le C_U Z_s. \tag{173}$$

Using (167) with $q = 2$ proves $U, H \in L^2$. The support contains only γ_1, γ_2, so uniform integrability in γ follows from (171). Theorem 1 applies up to τ.

For the full state space, take the exit times

$$\tau_n = \inf\{s \geq t : V_s \notin (1/n, n) \text{ or } r_s \notin (1/n, n)\} \wedge T. \tag{174}$$

The Feller conditions imply $\tau_n \uparrow T$ almost surely. If g_i, their logarithmic gradients, and the feedback have the stated polynomial growth and the family in (168) is uniformly integrable, the stopped identities pass to the limit by dominated convergence. This gives the full-state conclusion.

If Γ is degenerate at a single γ, then $M_0 = w$, $M_1 = \gamma w$, $M_v = \gamma w g_v/g$, and $M_r = \gamma w g_r/g$. It is convenient to set

$$\ell(t, v, r) = \gamma \log g(t, v, r). \tag{175}$$

The exposures become

$$\beta_S^* = \frac{\sqrt{v}}{\gamma}(\lambda_S - \sigma_{P1} + \rho\sigma_v \ell_v), \qquad \beta_P^* = \frac{\lambda_p - \sigma_{P2}}{\gamma}, \qquad \beta_r^* = \frac{\lambda_r \sqrt{r} + \chi\sigma_v \sqrt{v}\, \ell_v + \sigma_r \sqrt{r}\, \ell_r}{\gamma}. \tag{176}$$

Completing the three control squares in the logarithmic equation gives

$$\begin{aligned} 0 = {} & \ell_t + \kappa_v(\theta_v - v)\ell_v + \tfrac{1}{2}\sigma_v^2 v(\ell_{vv} + \ell_v^2) + \kappa_r(\theta_r - r)\ell_r + \tfrac{1}{2}\sigma_r^2 r(\ell_{rr} + \ell_r^2) \\ & + \chi\sigma_v\sigma_r \sqrt{vr}(\ell_{vr} + \ell_v\ell_r) + (1 - \gamma)(r - \eta) \\ & + \frac{1 - \gamma}{2\gamma}\Big[v(\lambda_S - \sigma_{P1} + \rho\sigma_v\ell_v)^2 + (\lambda_p - \sigma_{P2})^2 \\ & \qquad + (\lambda_r \sqrt{r} + \chi\sigma_v \sqrt{v}\, \ell_v + \sigma_r \sqrt{r}\, \ell_r)^2\Big], \qquad \ell(T, v, r) = 0. \end{aligned} \tag{177}$$

Corollary 1. *Let $\chi = 0$ and let Γ be degenerate. Suppose the following Riccati system has a finite solution on $[0, T]$. Then*

$$\ell(t, v, r) = A(t) + B(t)v + C(t)r \tag{178}$$

solves the fixed-γ problem, where $A(T) = B(T) = C(T) = 0$ and

$$0 = B' - \kappa_v B + \tfrac{1}{2}\sigma_v^2 B^2 + \frac{1 - \gamma}{2\gamma}(\lambda_S - \sigma_{P1} + \rho\sigma_v B)^2, \tag{179}$$

$$0 = C' - \kappa_r C + \tfrac{1}{2}\sigma_r^2 C^2 + (1 - \gamma) + \frac{1 - \gamma}{2\gamma}(\lambda_r + \sigma_r C)^2, \tag{180}$$

$$0 = A' + \kappa_v\theta_v B + \kappa_r\theta_r C - (1 - \gamma)\eta + \frac{1 - \gamma}{2\gamma}(\lambda_p - \sigma_{P2})^2. \tag{181}$$

Proof. For degenerate Γ with $\chi = 0$, equations (122)–(123) imply

$$\frac{M_0}{M_1} = \frac{1}{\gamma}, \qquad \frac{M_v}{M_1} = \frac{g_v}{g} = \frac{\ell_v}{\gamma}, \qquad \frac{M_r}{M_1} = \frac{g_r}{g} = \frac{\ell_r}{\gamma}. \tag{182}$$

This gives (176) with $\chi = 0$. For $\ell = A + Bv + Cr$,

$$\ell_t = A' + B'v + C'r, \qquad \ell_v = B, \quad \ell_r = C, \qquad \ell_{vv} = \ell_{vr} = \ell_{rr} = 0. \tag{183}$$

The three feedback exposures reduce to

$$\beta_S^* = \frac{\sqrt{v}}{\gamma}(\lambda_S - \sigma_{P1} + \rho\sigma_v B),$$
$$\beta_P^* = \frac{\lambda_p - \sigma_{P2}}{\gamma},$$
$$\beta_r^* = \frac{\sqrt{r}}{\gamma}(\lambda_r + \sigma_r C). \tag{184}$$

The stock terms involving β_S combine as

$$(1-\gamma)\beta_S(\lambda_S - \sigma_{P1})\sqrt{v} - \tfrac{1}{2}\gamma(1-\gamma)\beta_S^2 + (1-\gamma)\rho\sigma_v\sqrt{v}\beta_S B \tag{185}$$
$$= \frac{1-\gamma}{2\gamma}v(\lambda_S - \sigma_{P1} + \rho\sigma_v B)^2. \tag{186}$$

Similarly, the rate control terms become

$$\frac{1-\gamma}{2\gamma}r(\lambda_r + \sigma_r C)^2, \tag{187}$$

and the residual inflation terms become

$$\frac{1-\gamma}{2\gamma}(\lambda_p - \sigma_{P2})^2. \tag{188}$$

The remaining factor contributions are

$$\kappa_v(\theta_v - v)B + \tfrac{1}{2}\sigma_v^2 vB^2, \qquad \kappa_r(\theta_r - r)C + \tfrac{1}{2}\sigma_r^2 rC^2, \tag{189}$$

and the real short-rate term is $(1-\gamma)(r-\eta)$. Substitution of (183) and (184) in (177) therefore yields

$$\begin{aligned} 0 = {} & \left[A' + \kappa_v\theta_v B + \kappa_r\theta_r C - (1-\gamma)\eta + \frac{1-\gamma}{2\gamma}(\lambda_p - \sigma_{P2})^2\right] \\ & + v\left[B' - \kappa_v B + \frac{1}{2}\sigma_v^2 B^2 + \frac{1-\gamma}{2\gamma}(\lambda_S - \sigma_{P1} + \rho\sigma_v B)^2\right] \\ & + r\left[C' - \kappa_r C + \frac{1}{2}\sigma_r^2 C^2 + (1-\gamma) + \frac{1-\gamma}{2\gamma}(\lambda_r + \sigma_r C)^2\right]. \end{aligned} \tag{190}$$

Since $1, v, r$ are linearly independent on every open subset of $(0,\infty)^2$, each bracket in (190) vanishes. These three equations are exactly (179), (180), and (181). The terminal condition $\ell(T, v, r) = 0$ for every (v, r) gives $A(T) = B(T) = C(T) = 0$.

Proposition 4. *Let $\chi\sigma_v(\lambda_S - \sigma_{P1})\lambda_r \neq 0$ and let Γ be degenerate at $\gamma \neq 1$. Then the standard affine ansatz $\ell = A + Bv + Cr$ cannot solve the correlated fixed-γ equation on any interval immediately preceding T. Accordingly, the standard affine Riccati reduction is unavailable under these conditions, and the present analysis retains the two-dimensional continuation equation.*

Proof. Assume that $\ell = A + Bv + Cr$. Then $\ell_{vr} = 0$, and all terms in (177) are affine in (v, r) except terms proportional to $\sqrt{vr}$. The state covariation term contributes

$$\chi\sigma_v\sigma_r BC\,\sqrt{vr}. \tag{191}$$

In the final completed square of (177), the cross-product between $\chi\sigma_v B\,\sqrt{v}$ and $(\lambda_r+\sigma_r C)\,\sqrt{r}$ contributes

$$\frac{1-\gamma}{\gamma}\chi\sigma_v B(\lambda_r + \sigma_r C)\,\sqrt{vr}. \tag{192}$$

Consequently, the total coefficient of $\sqrt{vr}$ is

$$\chi\sigma_v B\left[\sigma_r C + \frac{1-\gamma}{\gamma}(\lambda_r + \sigma_r C)\right]. \tag{193}$$

An affine identity on an open subset of $(0,\infty)^2$ requires this coefficient to vanish at every time.

Write $\tau = T - t$. At $\tau = 0$, $B = C = 0$. The v coefficient in (177) gives

$$\left.\frac{\mathrm{d}B}{\mathrm{d}\tau}\right|_{\tau=0} = \frac{1-\gamma}{2\gamma}(\lambda_S - \sigma_{P1})^2 \neq 0. \tag{194}$$

Put $\Lambda_S = \lambda_S - \sigma_{P1}$ and write $B_\tau(0) = \mathrm{d}[B(T-\tau)]/\,\mathrm{d}\tau|_{\tau=0}$. The preceding identity gives

$$B(T-\tau) = \frac{1-\gamma}{2\gamma}\Lambda_S^2\tau + o(\tau), \qquad C(T-\tau) = O(\tau). \tag{195}$$

Hence, if $D(\tau)$ denotes the coefficient in (193) evaluated at $T-\tau$, then

$$\begin{aligned} D(\tau) &= \chi\sigma_v B(T-\tau)\left[\sigma_r C(T-\tau) + \frac{1-\gamma}{\gamma}(\lambda_r + \sigma_r C(T-\tau))\right] \\ &= \frac{\chi\sigma_v(1-\gamma)^2}{2\gamma^2}\Lambda_S^2\lambda_r\,\tau + o(\tau). \end{aligned} \tag{196}$$

Under $\chi\sigma_v\Lambda_S\lambda_r \neq 0$ and $\gamma \neq 1$, the coefficient in (196) is nonzero. Thus $D(\tau) \neq 0$ for all sufficiently small $\tau > 0$, contradicting the necessary affine identity $D(\tau) = 0$. Equation (193) gives the exceptional cases $\chi = 0$, $\sigma_v = 0$, $B = 0$, and the vanishing of its bracketed term; $\lambda_S - \sigma_{P1} = 0$ and $\lambda_r = 0$ give the corresponding terminal degeneracies. Hence the correlated fixed-γ equation has no solution of the form $A + Bv + Cr$. This proves the proposition.

4.3. Solution to the original problem

Using (78), the equilibrium risky fractions in the pension account are

$$\pi_j^*(t) = \frac{Y_t}{X_t}\phi_j^*(t) - \frac{F_t}{X_t}\pi_j^F(t) + \frac{G_t}{X_t}\pi_j^G(t), \qquad j \in \{S, N, I\}. \tag{197}$$

where $\pi_0^* = 1 - \pi_S^* - \pi_N^* - \pi_I^*$. The three terms in (197) are, respectively, the equilibrium allocation of total auxiliary wealth, the short position that offsets human capital, and the portfolio that immunizes the annuity guarantee.

Proposition 5. *Under the hypotheses of Proposition 3, the two-point equilibrium strategy* (197) *is admissible up to the localization time. Under the full-state growth and integrability hypotheses in the proof below, it is admissible on* $[0, T]$. *The same conclusion holds for a degenerate distribution when the correlated PDE solution satisfies the corresponding bounds; when* $\chi = 0$*, finiteness of the Riccati solution in Corollary 1 is sufficient on every stopped cylinder.*

Proof. Define the original risky dollar positions by

$$X_t \pi^*_{j,t} = Y_t \phi^*_{j,t} - F_t \pi^F_{j,t} + G_t \pi^G_{j,t}, \qquad j \in \{S, N, I\}. \tag{198}$$

This formulation remains meaningful even at a point where a fraction representation would divide by $X_t = 0$. Let $\mathcal{Y}_t = (X_t, Y_t, C_t, F_t, G_t)^\top$. On a stopped cylinder, the feedbacks and replication fractions are bounded and continuous. Substitution of (198) in (38), together with the SDEs for Y, C, F, G, V, r, yields

$$\mathrm{d}\mathcal{Y}_t = b(t, \mathcal{Y}_t, V_t, r_t)\,\mathrm{d}t + \Sigma(t, \mathcal{Y}_t, V_t, r_t)\,\mathrm{d}\widetilde{W}_t, \tag{199}$$

where $\widetilde{W} = (W_1, W_2, W_3, W_4)^\top$ and, for a constant $C_D < \infty$,

$$|b(t, y, v, r) - b(t, \tilde{y}, v, r)| + |\Sigma(t, y, v, r) - \Sigma(t, \tilde{y}, v, r)| \le C_D |y - \tilde{y}|, \tag{200}$$

$$|b(t, y, v, r)| + |\Sigma(t, y, v, r)| \le C_D(1 + |y|). \tag{201}$$

Thus (199) has a unique strong solution. Moreover, the real auxiliary wealth has the explicit representation

$$Z_s = Z_t \mathcal{E}\left(\int_t^s (\beta^*_u)^\top \,\mathrm{d}W_u\right) \exp\left\{\int_t^s [r_u - \eta + (\beta^*_u)^\top \theta_u]\,\mathrm{d}u\right\} > 0, \qquad s \le T \wedge \tau. \tag{202}$$

By construction, $Y_T = X_T - G_T$ and (202) gives $Y_T = P_T Z_T > 0$; hence $X_T > G_T$ almost surely. The original and auxiliary criteria coincide by (76). For the two-point case, we have

$$V(t, z, v, r) = z[p_1 w_1(t, v, r) + p_2 w_2(t, v, r)], \tag{203}$$

which is finite under the bounds in Proposition 3. Equations (167), (170), and (173) imply that every localized stochastic integral used in the criterion and verification argument is a true martingale. Thus the integrability condition in Definition 1 holds. Passing from stopped cylinders to the full state space uses the same localization and uniform integrability argument as in the proof of Proposition 3. For a degenerate distribution with $\chi \neq 0$, the identical proof applies under the stated PDE bounds. In the nested case $\chi = 0$, the finiteness of the Riccati solution bounds the affine exponent on every stopped cylinder.

5. Numerical analysis

5.1. Parameterization and numerical method

The experiment uses a 30-year horizon, $\gamma_1 = 0.5$, and $\gamma_2 = 4$. The balanced case has $(p_1, p_2) = (0.5, 0.5)$, while the case weighted by low risk aversion has $(0.8, 0.2)$. These two cases vary both the mean and the distribution. A separate same-mean experiment below isolates dispersion. Table 2 reports

the baseline annualized parameters. Both Feller conditions hold: $2\kappa_v\theta_v = 0.12 > 0.0225 = \sigma_v^2$ and $2\kappa_r\theta_r = 0.015 > 0.0016 = \sigma_r^2$. The correlation matrix of the stock, variance, and short-rate shocks is

$$\begin{pmatrix} 1 & \rho & 0 \\ \rho & 1 & \chi \\ 0 & \chi & 1 \end{pmatrix}, \tag{204}$$

whose eigenvalues at $(\rho, \chi) = (-0.60, -0.25)$ are 0.35, 1, and 1.65. Hence the joint loading restriction is satisfied with a nontrivial margin.

Table 2. Baseline parameters.

Parameter	Value	Interpretation	Parameter	Value	Interpretation
T	30	Horizon	V_0	0.040	Initial variance
κ_v	1.50	Variance reversion	θ_v	0.040	Long-run variance
σ_v	0.150	Volatility of variance	ρ	−0.60	Return–variance correlation
χ	−0.25	Variance–rate correlation	λ_S	0.80	Equity-risk price
r_0	0.025	Initial short rate	κ_r	0.25	Rate reversion
θ_r	0.030	Long-run short rate	σ_r	0.040	Rate volatility
λ_r	0.15	Rate-risk price	η	0.014	Pricing inflation drift
σ_{P1}	0.150	Stock inflation loading	σ_{P2}	0.015	Residual inflation volatility
λ_p	−0.020	Inflation-risk price			

Table 2 sets the baseline correlation at $\chi = -0.25$ and evaluates the range $[-0.45, 0.25]$. Ballestra et al. [22] reported rolling correlations from approximately −0.63 to 0.63 between volatility series constructed from S&P 500 returns and 3-month Treasury bill rate changes over 1975–2022. The reported discrete-time proxy correlations set the scale of the sensitivity range. The instantaneous loading χ is specified as a structural parameter of the Heston–CIR dynamics, and the selected range evaluates negative, zero, and positive variance–rate dependence in the equilibrium system. The risk aversion distributions specify theoretical parameter cases for the model comparisons; no survey, administrative, or market data are used to estimate them. The numerical quantities below are therefore parameter study outcomes for the stated inputs.

The numerical analysis uses the log form $\ell_i = \gamma_i \log g_i$, which is algebraically equivalent to (127). With time to maturity $\tau = T - t$, the baseline domain

$$v \in [0.004, 0.14], \qquad r \in [0.002, 0.09] \tag{205}$$

is evaluated at a 37×37 spatial resolution with $\Delta\tau = 0.0015$. Section 5.7 examines temporal and spatial resolution, the state domain, alternative boundary specifications, and an independent high-resolution calculation.

For the policy transfer experiment, the true-χ equilibrium criterion, the restricted $\chi = 0$ equilibrium, and the continuation value of the restricted feedback under the true generator are evaluated under the same temporal resolution, spatial resolution, state domain, and boundary specification. Each reported policy value difference is therefore formed under a common numerical specification.

5.2. Equilibrium exposures and the risk aversion distribution

Figure 1 shows the balanced equilibrium along (V_0, r_0). The plotted quantities are Brownian exposures of real auxiliary wealth. They should not be confused with asset fractions, which follow (128)–(130). Throughout the numerical section, stock, short rate, and residual inflation exposure refer only to the components of β. The symbols ϕ and π are reserved for auxiliary wealth and original account fractions, respectively.

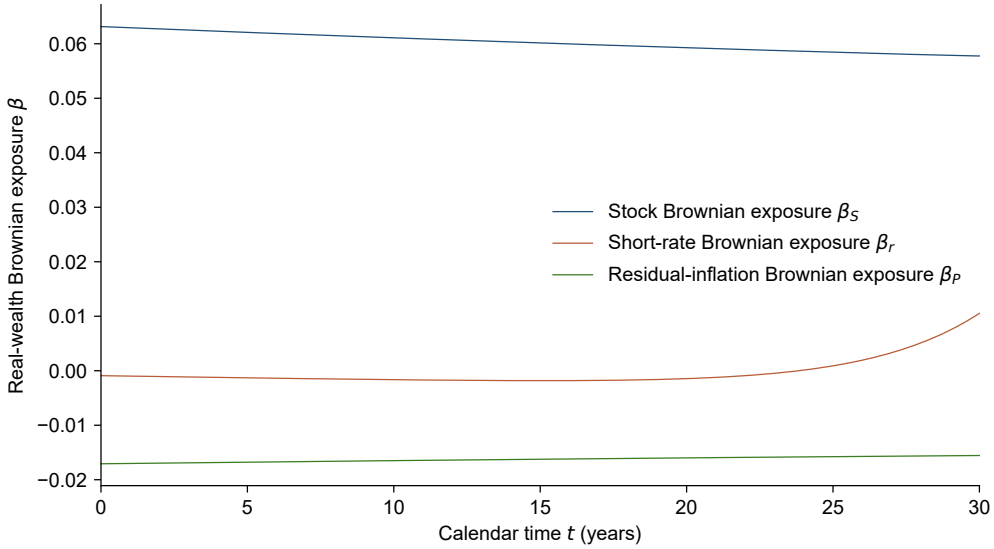


Figure 1. Equilibrium real wealth Brownian exposures for $p_1 = p_2 = 0.5$, evaluated at $V = 0.04$ and $r = 0.025$.

At time zero, the balanced stock Brownian exposure is 0.063155 and the net short rate Brownian exposure is slightly negative. The residual inflation Brownian exposure is negative because $\lambda_p - \sigma_{P2} = -0.035$. At retirement, the continuation gradients vanish, so the new cross-hedge also vanishes. Equations (124)–(126) therefore reduce to

$$\beta_S^* = \frac{(\lambda_S - \sigma_{P1})\sqrt{v}}{\mathbb{E}[\gamma]}, \quad \beta_P^* = \frac{\lambda_p - \sigma_{P2}}{\mathbb{E}[\gamma]}, \quad \beta_r^* = \frac{\lambda_r \sqrt{r}}{\mathbb{E}[\gamma]}, \tag{206}$$

and the terminal entries in Table 3 agree to the reported precision.

Table 3. Equilibrium real wealth Brownian exposures at the initial and terminal dates.

Distribution	Date	β_S^*	β_r^*	β_P^*
$p_1 = 0.5$	$t = 0$	0.063155	−0.000908	−0.017073
$p_1 = 0.5$	$t = T$	0.057762	0.010538	−0.015556
$p_1 = 0.8$	$t = 0$	0.169441	0.040865	−0.047332
$p_1 = 0.8$	$t = T$	0.108303	0.019759	−0.029167

Figure 2 compares the two distributions. Raising the probability of $\gamma_1 = 0.5$ increases all risk-tolerance-driven positions in magnitude. At time zero, the stock Brownian exposure rises from 0.063155

to 0.169441, while the short rate Brownian exposure changes from −0.000908 to 0.040865. These changes cannot be reconstructed from the arithmetic mean alone because w_i, M_v, and M_r evolve jointly through the coupled continuation equations.

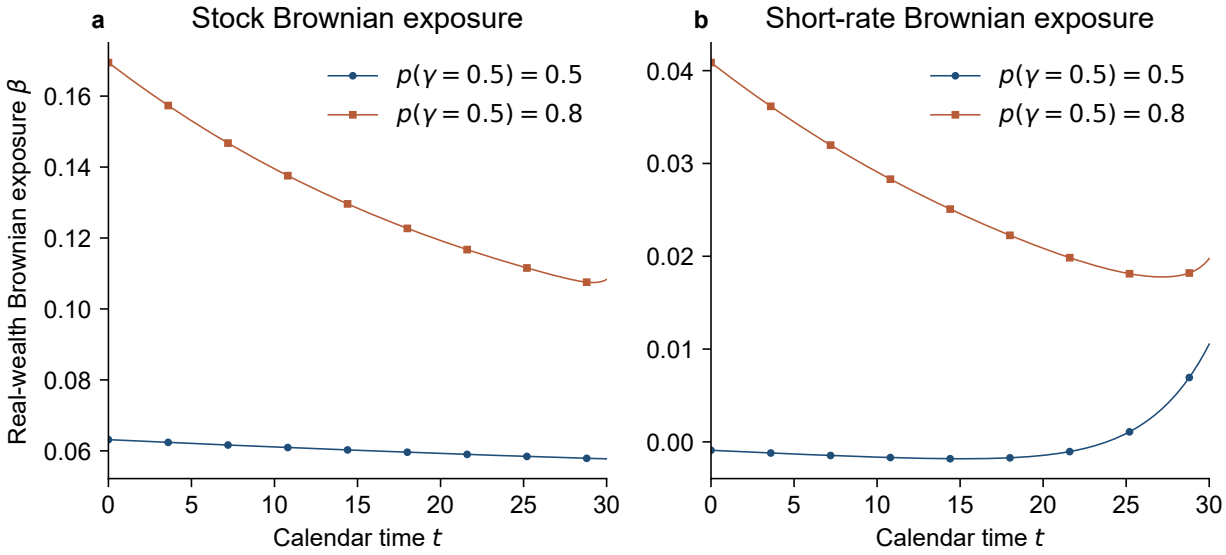


Figure 2. Brownian exposures under alternative risk aversion distributions.

5.3. Implementable original account portfolio

The auxiliary Brownian exposures are intermediate quantities. We therefore evaluate the original account strategy in (197). Table 4 supplies the contribution, annuity, and bond inputs that do not enter the normalized auxiliary problem. The ratios $X_t/P_t = 1$ and $C_t/P_t = 0.03$ define a common conditional reference state at each date. This normalization makes the state dependence of the implementable mapping transparent.

Table 4. Additional inputs for the original account portfolio.

Parameter	Value	Parameter	Value
Contribution growth μ	0.030	Contribution ratio C_t/P_t	0.030
Contribution loading σ_{C1}	0.100	Contribution loading σ_{C2}	0.006
Initial annuity rate $a(T)$	0.040	Annuity growth a_0	0.000
Maximum lifetime ω	55	Reference wealth X_t/P_t	1.000
Nominal bond maturity K_N	10 years	Indexed bond maturity K_I	10 years

For these inputs, $d(t,s,r) = e^{\mu(s-t)}A_N(s-t)e^{-B_N(s-t)r}$, and the loading of each 10-year rolling bond is $b_N = b_I = -0.143044$. The resulting claim ratios F_t/X_t, G_t/X_t, and $Y_t/X_t = 1 + F_t/X_t - G_t/X_t$ enter the original account mapping in Proposition 2. The corresponding implementable fractions are reported in Table 5.

The fractions sum to one at every reported date. At time zero, future contributions raise auxiliary wealth to 1.638969 times current pension wealth. The resulting stock demand is partly financed by short nominal and indexed bond positions. As retirement approaches, human capital falls and the guarantee becomes more prominent. The nominal and indexed bond fractions therefore move from negative to

positive in the reported reference states. These are conditional policy values; other account, contribution, variance, and rate states are obtained directly from (197).

Table 5. Conditional original account fractions in the balanced case at $(V_t, r_t) = (0.04, 0.025)$.

t	F_t/X_t	G_t/X_t	Y_t/X_t	π_S^*	π_N^*	π_I^*	π_0^*
0	0.926118	0.287149	1.638969	0.760329	−0.188437	−0.309858	0.737966
10	0.613606	0.333438	1.280167	0.577635	−0.045199	−0.039626	0.507190
20	0.304468	0.387095	0.917373	0.406358	0.051033	0.204874	0.337735

5.4. Same-mean preference heterogeneity and support robustness

The earlier probability comparison changes both the arithmetic mean and higher moments of risk aversion. To isolate dispersion, Table 6 uses three symmetric two-point distributions with common mean 2.25. Each equilibrium is compared with the same fixed coefficient $\bar{\gamma} = 2.25$. The effective coefficient $\varepsilon(t, V_0, r_0)$ is reported at four dates.

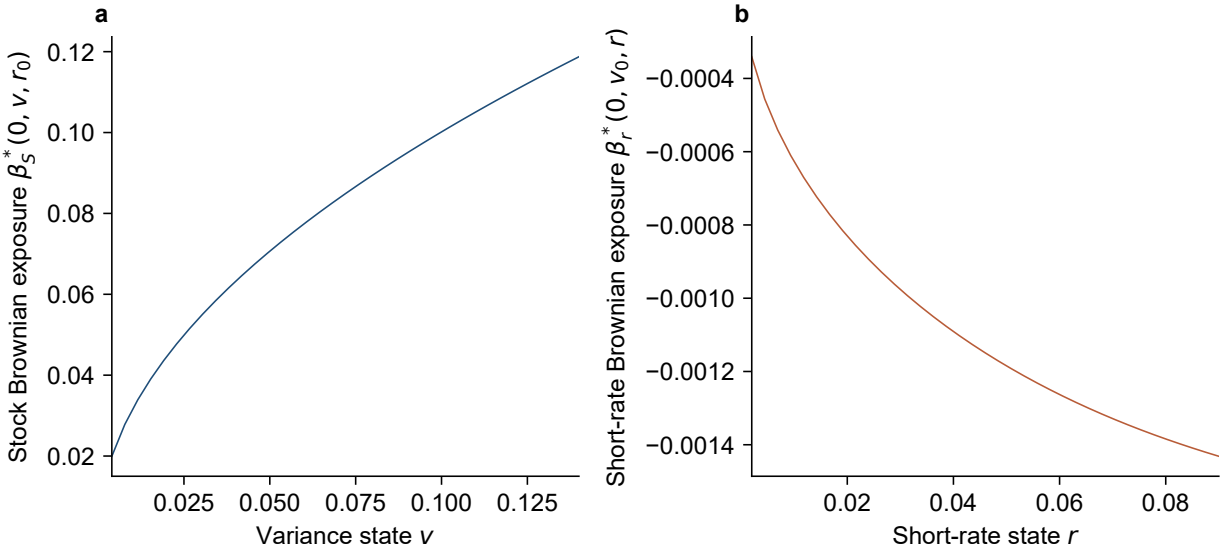


Figure 3. Initial state dependence of stock and short rate Brownian exposures in the balanced case.

Table 6. Same-mean dispersion, effective risk aversion, initial Brownian exposures, and loss under the mean risk aversion policy.

Support	Var(γ)	$\varepsilon(0)$	$\varepsilon(10)$	$\varepsilon(20)$	$\varepsilon(T)$	$\beta_S^*(0)$	$\beta_r^*(0)$	Loss (%)
{1.50, 3.00}	0.5625	2.215280	2.227173	2.238892	2.250000	0.059175	−0.002693	0.0010
{0.50, 4.00}	3.0625	2.049962	2.121807	2.189120	2.250000	0.063155	−0.000908	0.0325
{0.25, 4.25}	4.0000	1.982469	2.080477	2.170282	2.250000	0.064937	−0.000082	0.0580

Greater dispersion lowers the effective coefficient away from retirement in this parameterization. It also raises the initial stock Brownian exposure and the loss from replacing the distribution by its mean.

All three effective coefficients converge to 2.25 at retirement because $g_i(T) = 1$ makes the monetary weights equal to their probabilities. The pattern demonstrates a dispersion effect at a fixed mean, but it is not asserted as a parameter-free monotonicity result.

Figure 3 reports the complete time paths rather than only the four dates in Table 6. The fixed-mean benchmark $\delta_{2.25}$ is constant at 2.25. Before retirement, the separation from that benchmark is larger for the more dispersed distributions and closes continuously at T.

To check whether the narrow two-point result is driven by support cardinality, we also use the three-point law

$$\Gamma_3 = \{(0.50, 9/98), (2.25, 40/49), (4.00, 9/98)\}. \tag{207}$$

It has the same mean 2.25 and variance 0.5625 as the equal-probability two-point law on $\{1.50, 3.00\}$, but different higher moments. Table 7 shows that the initial effective coefficient differs by 2.17×10^{-5}, the stock exposure by 4.30×10^{-7}, the rate exposure by 4.95×10^{-7}, and the welfare loss by 2.66×10^{-6} percentage points. Thus support cardinality has no material effect in this matched moment experiment. The three-point calculation provides numerical robustness evidence for the finite-support extension.

Table 7. Matched moment robustness to a three-point risk aversion distribution.

Distribution	$\varepsilon(0)$	$\beta_S^*(0)$	$\beta_r^*(0)$	J^*	Loss (%)
Two-point	2.215280	0.05917521	−0.00269320	1.77481956	0.00098764
Three-point	2.215258	0.05917564	−0.00269271	1.77482032	0.00099030

5.5. *Heston and CIR state dependence*

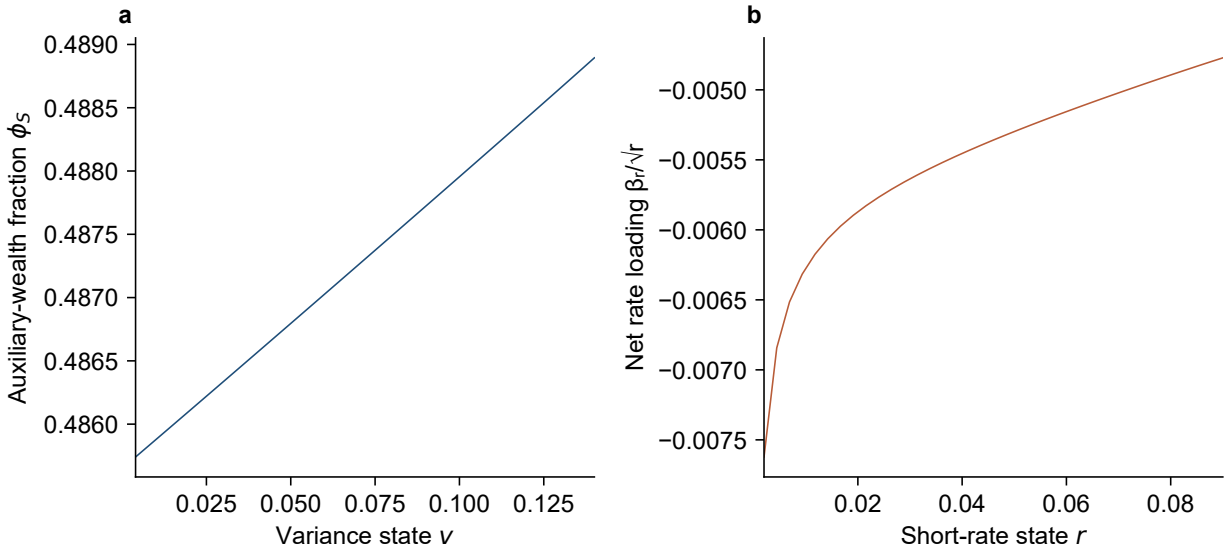


Figure 4. State-normalized portfolio positions.

Figure 3 plots the initial stock and short rate Brownian exposures over their state grids. Figure 4 converts the stock Brownian exposure into the auxiliary wealth stock fraction. From $L\phi = \beta + \sigma_P$, we have

$$\phi_S = \frac{\beta_S}{\sqrt{v}} - \frac{\sigma_{P1}}{\sigma_{P2}}\beta_P. \tag{208}$$

The dependence remaining after the mechanical $\sqrt{v}$ scale is the Heston hedging component and the endogenous certainty equivalent weight.

Return–variance correlation enters both the direct hedge $\rho\sigma_v M_v/M_1$ and the continuation equations. Table 8 shows that moving ρ from -0.8 to 0 raises the initial stock exposure from 0.063046 to 0.063505 for this parameterization. The effect is smaller than the distributional change in Figure 2; this ranking is model- and parameter-dependent.

Table 8. Initial Brownian exposure sensitivity to return–variance correlation.

ρ	β_S^*	β_r^*	β_P^*
−0.80	0.063046	−0.000919	−0.017064
−0.60	0.063155	−0.000908	−0.017073
−0.30	0.063325	−0.000891	−0.017088
0.00	0.063505	−0.000873	−0.017102

Figure 5 displays the same return–variance-correlation comparison over the full reported range.

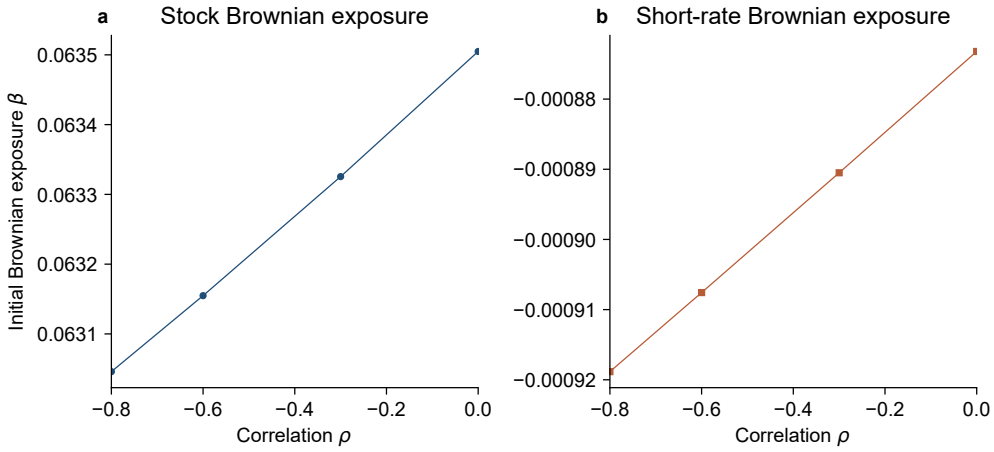


Figure 5. Initial Brownian exposures as functions of return–variance correlation.

Table 9. Initial Brownian exposure and criterion sensitivity to variance–rate correlation.

χ	β_S^*	β_r^*	β_P^*	J^*
−0.45	0.063143	−0.000995	−0.017070	1.779710
−0.25	0.063155	−0.000908	−0.017073	1.779852
0.00	0.063170	−0.000796	−0.017078	1.780034
0.25	0.063185	−0.000684	−0.017083	1.780222

The new parameter χ acts differently from ρ. It enters the variance–rate state covariance, the continuation PDE, and the short rate Brownian exposure directly through $\chi\sigma_v\sqrt{v}\,M_v/M_1$. Table 9 isolates this channel while holding every other parameter fixed. Raising χ from -0.45 to 0.25 increases the initial short rate Brownian exposure from -0.000995 to -0.000684. The stock and residual inflation

Brownian exposures move only slightly, while the criterion increases monotonically over the baseline parameter range.

The endpoint change in β_r^* is 0.000311852, or 31.3% of its magnitude at $\chi = -0.45$. A more direct policy experiment fixes the true dynamics at $\chi = -0.25$, computes the full equilibrium feedback under the misspecified restriction $\chi = 0$, and evaluates that feedback under the true generator. Let J_χ^* denote the exact correlated equilibrium criterion and let $J_\chi^{(0)}$ denote the criterion of the $\chi = 0$ feedback under the same true χ dynamics. We report the signed equivalent initial wealth difference

$$\Delta_\chi = 100\left(1 - \frac{J_\chi^{(0)}(0, 1, V_0, r_0)}{J_\chi^*(0, 1, V_0, r_0)}\right). \tag{209}$$

Table 10 reports the exact policy and transferred policy comparison under the common baseline dynamics.

Table 10. Policy transfer experiment under the true baseline dynamics $\chi = -0.25$.

Policy	$\beta_S(0)$	$\beta_r(0)$	$\beta_P(0)$	Criterion	Δ_χ (%)
Exact $\chi = -0.25$ equilibrium	0.06315484	−0.00090757	−0.01707349	1.77985191	0
$\chi = 0$ feedback, true $\chi = -0.25$	0.06317002	−0.00079636	−0.01707802	1.77985714	−0.000294

Under the baseline parameterization, suppressing correlation changes the initial rate exposure by 12.3% relative to the exact baseline magnitude. Table 11 recomputes the direct difference under time and space refinement, domain expansion, an alternative boundary specification, and homogeneous Neumann data. Although the Neumann rule shifts the individual criterion by about 9.76×10^{-5}, $J_\chi^{(0)} - J_\chi^*$ remains positive and lies between 5.2362×10^{-6} and 5.2918×10^{-6} across all eight specifications; equivalently, Δ_χ lies between −0.00029733% and −0.00029419%. The signed ordering is therefore numerically stable in these checks, but its economic magnitude is negligible; the visible policy effect is the reallocation of the rate exposure.

Table 11. Direct policy value difference under common numerical specifications.

Specification	J_χ^*	$J_\chi^{(0)}$	$10^6[J_\chi^{(0)} - J_\chi^*]$	Δ_χ (%)
Time, coarse	1.779851743	1.779856980	5.236841	−0.000294229
Baseline	1.779851907	1.779857144	5.236641	−0.000294218
Time, fine	1.779851989	1.779857226	5.236541	−0.000294212
Space, coarse	1.779851968	1.779857206	5.238052	−0.000294297
Space, fine	1.779851994	1.779857230	5.236202	−0.000294193
Expanded domain	1.779851969	1.779857205	5.236537	−0.000294212
Alternative boundary	1.779851971	1.779857207	5.236238	−0.000294195
Homogeneous Neumann	1.779754369	1.779759661	5.291792	−0.000297333

The affine approximations of Grzelak and Oosterlee [20] are defined for derivative pricing transforms. We introduce an explicit closure for the endogenous ratios M_v/M_1 and M_r/M_1 and evaluate the comparison in the degenerate case $\Gamma = \delta_4$, where the system reduces to one logarithmic PDE. This deterministic projection is a surrogate for the degenerate preference single-PDE problem; the full random preference model remains governed by the exact coupled system.

Let $\tau = T - t$, and define deterministic physical mean states and their product projection by

$$\bar{v}(t) = \theta_v + (V_0 - \theta_v)e^{-\kappa_v t}, \qquad \bar{r}(t) = \theta_r + (r_0 - \theta_r)e^{-\kappa_r t}, \qquad q_{\mathrm{pr}}(t) = \sqrt{\bar{v}(t)\bar{r}(t)}. \tag{210}$$

For the affine candidate $\ell_{\mathrm{pr}} = A + Bv + Cr$, the only nonaffine contribution in (177) is $\Xi(B, C)\sqrt{vr}$, where

$$\Xi(B, C) = \chi\sigma_v B\left[\sigma_r C + \frac{1-\gamma}{\gamma}(\lambda_r + \sigma_r C)\right]. \tag{211}$$

Replacing only $\sqrt{vr}$ by $q_{\mathrm{pr}}(t)$ yields the time-inhomogeneous affine system below, with dots denoting derivatives in τ and $A(0) = B(0) = C(0) = 0$:

$$\begin{aligned}
\dot{B} &= -\kappa_v B + \tfrac{1}{2}\sigma_v^2 B^2 + \frac{1-\gamma}{2\gamma}\left[(\lambda_S - \sigma_{P1} + \rho\sigma_v B)^2 + (\chi\sigma_v B)^2\right],\\
\dot{C} &= -\kappa_r C + \tfrac{1}{2}\sigma_r^2 C^2 + (1-\gamma) + \frac{1-\gamma}{2\gamma}(\lambda_r + \sigma_r C)^2,\\
\dot{A} &= \kappa_v\theta_v B + \kappa_r\theta_r C - (1-\gamma)\eta + \frac{1-\gamma}{2\gamma}(\lambda_p - \sigma_{P2})^2 + \Xi(B, C)q_{\mathrm{pr}}(T-\tau).
\end{aligned} \tag{212}$$

The $(\chi\sigma_v B)^2$ term is retained in the B equation. Thus the approximation projects precisely the obstruction in Proposition 4, rather than deleting variance–rate dependence.

Table 12 compares this stated surrogate with the exact correlated PDE on the 49×49 grid at $\Delta\tau = 0.00075$. The initial certainty-equivalent difference is 0.001174%, and the largest absolute log-value discrepancy over the full grid is 1.18×10^{-4}. These values quantify the stated projection at the reported parameterization.

Table 12. Exact correlated PDE and deterministic-projection affine surrogate for $\Gamma = \delta_4$ and $\chi = -0.25$.

Quantity	Exact PDE	Projection	Error
$\ell(0, V_0, r_0)$	−1.53807109	−1.53810630	3.52×10^{-5}
Initial certainty equivalent	1.66977746	1.66979706	0.001174%
Full-grid maximum log error	–	–	1.18×10^{-4}
Full-grid root mean square (RMS) log error	–	–	5.51×10^{-5}

Table 13 decomposes the numerator of (130). The four entries are the myopic rate demand λ_r/ε, the variance–rate cross-hedge, the CIR duration hedge, and the offset $-b_I\phi_I^*$. Their sum is divided by $b_N = -0.143044$ to obtain the auxiliary nominal bond fraction. At the baseline $\chi = -0.25$, $M_v/M_1 = 0.013528 > 0$. The negative correlation therefore makes the cross-hedge negative. It changes sign when χ becomes positive.

Table 13. Decomposition of the initial auxiliary nominal bond demand.

χ	Myopic	Cross-hedge	Duration hedge	Indexed offset	Numerator	ϕ_N^*
−0.45	0.073157	−0.001149	−0.078306	−0.019739	−0.026037	0.182024
−0.25	0.073172	−0.000642	−0.078272	−0.019773	−0.025515	0.178374
0.00	0.073192	0.000000	−0.078230	−0.019817	−0.024855	0.173757
0.25	0.073211	0.000650	−0.078187	−0.019861	−0.024186	0.169080

The cross-term is small relative to the myopic and duration components, but those larger components nearly offset each other. The cross-hedge is therefore visible in the residual numerator and in ϕ_N^*. Table 14 varies the volatility of variance, rate volatility, and the nominal bond maturity. Increasing σ_v from 0.12 to 0.18 increases the magnitude of the cross-hedge from 0.000520 to 0.000760. Rate volatility has a smaller direct effect on the cross-term, but it materially changes the duration hedge and the bond loading. A longer nominal bond maturity increases $|b_N|$ and reduces the fraction required to deliver a given rate loading.

Table 14. Sensitivity of the cross-hedge and the auxiliary nominal bond fraction.

Scenario	Cross-hedge	Duration hedge	b_N	ϕ_N^*
$\sigma_v = 0.12$	−0.000520	−0.078240	−0.143044	0.177516
$\sigma_v = 0.18$	−0.000760	−0.078304	−0.143044	0.179210
$\sigma_r = 0.03$	−0.000624	−0.059675	−0.108144	0.017877
$\sigma_r = 0.05$	−0.000662	−0.096036	−0.177225	0.273320
$K_N = 5$ years	−0.000642	−0.078272	−0.112406	0.226991
$K_N = 15$ years	−0.000642	−0.078272	−0.151328	0.168609
$K_N = 20$ years	−0.000642	−0.078272	−0.153563	0.166155

Figure 6 summarizes the exposure responses to the variance–rate correlation.

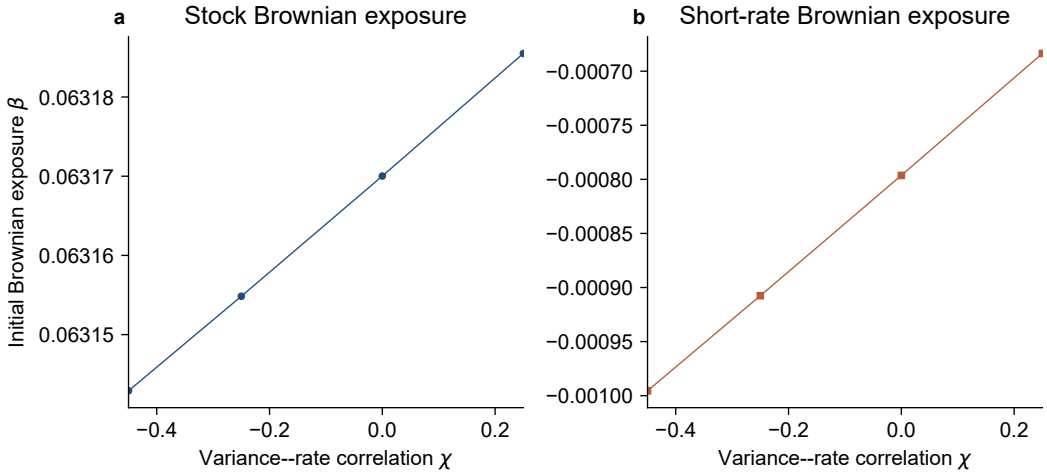


Figure 6. Initial Brownian exposures as functions of the variance–rate correlation.

5.6. Welfare loss

As in the benchmark, we compare the equilibrium with the fixed-$\bar{\gamma}$ policy obtained by substituting $\bar{\gamma} = \mathbb{E}[\gamma]$ for the random coefficient. We evaluate this policy for each actual γ_i under the original random preference criterion rather than under its own utility.

At unit initial real auxiliary wealth, we have

$$J^*(0, 1, V_0, r_0) = \sum_i p_i w_i^*(0, V_0, r_0). \tag{213}$$

Let $\bar{J}$ be the same criterion under the fixed-$\bar{\gamma}$ policy. Homogeneity implies that the equivalent initial wealth loss is

$$\delta = 1 - \frac{\bar{J}(0, 1, V_0, r_0)}{J^*(0, 1, V_0, r_0)}. \tag{214}$$

Table 15 reports the equivalent initial wealth loss for the three probability cases.

Table 15. Welfare loss from replacing random risk aversion by its mean.

Distribution	$\mathbb{E}[\gamma]$	J^*	$\bar{J}$	Loss (%)
$p_1 = 0.5$	2.25	1.779852	1.779273	0.0325
$p_1 = 0.8$	1.20	2.095866	2.057066	1.8513

Figure 7 shows the corresponding loss over the full horizon.

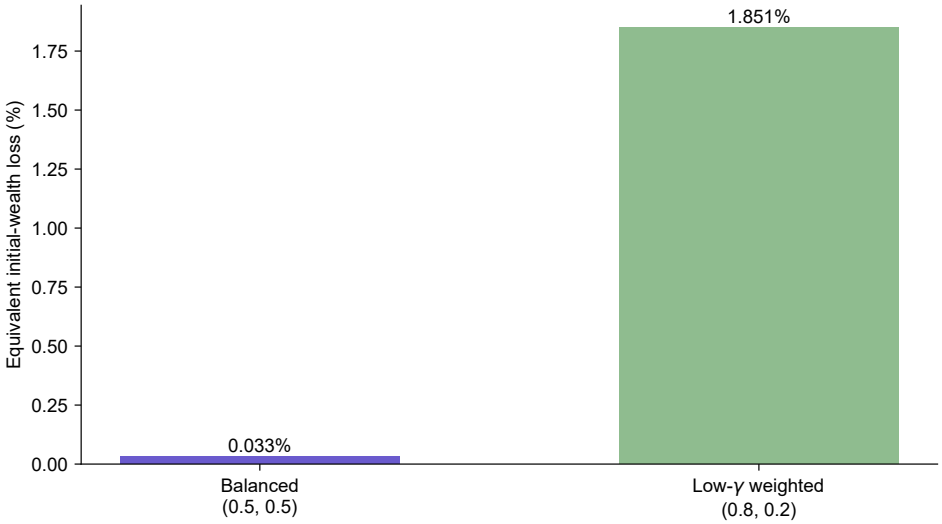


Figure 7. Equivalent initial wealth loss under the mean risk aversion policy.

The balanced distribution produces a small but positive loss. When the low risk aversion state has probability 0.8, the loss rises to 1.8513%. The difference is generated by the nonlinear monetary weights and by their interaction with variance and rate gradients over the full horizon.

5.7. Numerical checks

Table 16 reports temporal and spatial refinement, an expanded state rectangle $[0.002, 0.18] \times [0.001, 0.12]$, an alternative boundary specification, and homogeneous Neumann data on every artificial face.

Across the reported spatial resolutions, the initial stock and short rate Brownian exposures vary by less than 2.70×10^{-5} and 3.81×10^{-7}. Expanding the state domain changes these quantities by 5.24×10^{-6} and 2.24×10^{-8} relative to the fine-time baseline. The alternative boundary specification changes both displayed exposures by less than 10^{-10}. More stringently, the homogeneous Neumann condition sets $\ell_{i,v} = 0$ at $v \in \{0.004, 0.14\}$ and $\ell_{i,r} = 0$ at $r \in \{0.002, 0.09\}$. Relative to the fine-time baseline, it changes β_S^* by 1.61×10^{-7}, β_r^* by 3.97×10^{-6}, and the criterion by 9.76×10^{-5}. This alternative

boundary condition is retained as a sensitivity result rather than substituted for the baseline. At the common coarse specification, the independent calculation differs from the baseline by 5.29×10^{-10} in β_S^*, 2.17×10^{-10} in β_r^*, and 1.95×10^{-10} in the criterion. Increasing the independent spatial resolution from 37×37 to 101×101 changes the initial stock exposure by 1.52×10^{-5}, the rate exposure by 2.83×10^{-7}, and the criterion by 5.71×10^{-9}. Relative to the reported 49×49 calculation, the 101×101 independent values differ by 5.99×10^{-6}, 1.80×10^{-7}, and 2.43×10^{-7}, respectively. The residual inflation Brownian exposure remains stable to the displayed precision.

Table 16. Temporal, spatial, domain, and boundary sensitivity checks for the balanced case.

Check	Resolution/domain/ boundary	$\Delta\tau$	β_S^*	β_r^*	J^*
Time, coarse	37×37, baseline domain/boundary	0.00300	0.063154812	−0.000907590	1.779851743
Baseline	37×37, baseline domain/boundary	0.00150	0.063154840	−0.000907572	1.779851907
Time, fine	37×37, baseline domain/boundary	0.00075	0.063154854	−0.000907563	1.779851989
Space, coarse	25×25, baseline domain/boundary	0.00075	0.063137091	−0.000907314	1.779851968
Space, fine	49×49, baseline domain/boundary	0.00075	0.063164043	−0.000907693	1.779851994
Domain	49×49, expanded domain	0.00075	0.063160076	−0.000907586	1.779851969
Alternative boundary	37×37, alternative boundary	0.00075	0.063154854	−0.000907563	1.779851971
Neumann	37×37, homogeneous Neumann	0.00075	0.063154693	−0.000911533	1.779754369
Independent check	37×37, baseline domain/boundary	0.00300	0.063154813	−0.000907589	1.779851744
Independent high resolution	101×101, baseline domain/boundary	0.00300	0.063170035	−0.000907873	1.779851750

Table 17. Robustness of the variance–rate correlation comparative static.

Specification	$\beta_r^*(\chi=-0.45)$	$\beta_r^*(\chi=0.25)$	Difference
Baseline	−0.000995478	−0.000683625	0.000311852
Fine time step	−0.000995469	−0.000683616	0.000311853
Expanded domain	−0.000995498	−0.000683622	0.000311876
Homogeneous Neumann	−0.000999398	−0.000687743	0.000311654

Table 17 repeats the two endpoints of the χ comparison under time refinement, domain expansion, and homogeneous Neumann data. The increase in $\beta_r^*(0)$ lies between 3.1165×10^{-4} and 3.1188×10^{-4} across these specifications. Its sign and economic scale are stable across the baseline time step, state rectangle, and tested artificial boundary treatment.

The numerical findings also connect back to the institutional motivation. Preference dispersion shows that a representative risk aversion coefficient can obscure differences in the members' tolerance for market risk. The guarantee imposes a protection constraint on market-based accumulation, while the recovered hedging positions distinguish return-seeking from the management of inflation, interest rate, and variance shocks. These mechanisms make the modeled allocation and management of pension risk explicit. This feature connects the analysis to political economy research on pension financialization and the transfer of market risk to households [10, 12]. The connection is interpretive rather than evaluative. Because the study is not calibrated to China, it does not measure coverage, redistribution, class relations, contribution burdens, or common prosperity outcomes.

6. Conclusion

This paper integrates random risk aversion equilibrium with protected DC replication in a correlated Heston–CIR market. Future contributions and the inflation-linked annuity guarantee are priced and replicated before optimization, converting the pension account into self-financing real auxiliary wealth. A spike deviation argument verifies the coupled equilibrium system under the stated regularity, admissibility, and integrability conditions. The finite two-point system has a local classical solution on a stopped positive state rectangle. For a general distribution, the continuation equations provide an aggregate feedback fixed-point characterization conditional on a positive classical solution.

Variance–rate correlation creates the implementable rate-side variance hedge $\chi\sigma_v\sqrt{v/r}\,M_v/M_1$, alongside the stock-side variance hedge and the CIR duration hedge. It also generates the mixed derivative in the continuation equations. In the degenerate preference problem, the resulting $\sqrt{vr}$ coefficient excludes the standard ansatz $A+Bv+Cr$ under the nondegeneracy conditions of Proposition 4. The deterministic projection in (210)–(212) is an affine surrogate only for this degenerate preference continuation equation, not for the full random preference system, and has an initial certainty-equivalent error of 0.001174% for the stated parameter case.

The numerical evidence supports the comparative statics. Temporal and spatial refinement, domain expansion, alternative boundary specifications, and an independent high-resolution calculation leave the reported controls stable. The correlation effect from $\chi = -0.45$ to 0.25 also remains stable across the reported specifications, including the Neumann condition. At the baseline, the cross-hedge component is -0.000642 in the nominal bond numerator. Applying the $\chi = 0$ feedback under the true $\chi = -0.25$ dynamics changes the initial rate exposure by 12.3%. Direct matched comparisons across eight numerical specifications give $J_\chi^{(0)} - J_\chi^* \in [5.2362, 5.2918] \times 10^{-6}$ and $\Delta_\chi \in [-0.00029733, -0.00029419]\%$. The signed ordering is stable in these checks, but the value effect is economically negligible and is not interpreted as economically material policy dominance. The original account calculation converts the auxiliary solution into stock, nominal bond, indexed bond, and cash fractions at three reference dates. Same-mean distributions show that greater preference dispersion lowers effective risk aversion before retirement and raises the welfare loss in this parameterization. A matched-moment three-point distribution leaves the narrow two-point result essentially unchanged.

The exact replication and reduction in protected wealth apply under the imposed Heston-compatible common loading structure. Under this structure, the three claim shocks are replicated while the W_3 driven idiosyncratic variance risk remains unspanned. The resulting equilibrium system traces each variance–rate correlation term from Brownian loadings through claim valuation, verification, portfolio recovery, and numerical analysis. The reported parameterization quantifies these channels across the stated state space and preference distributions.

These mathematical results also have a bounded institutional implication. Pension assets represent deferred resources for retirement consumption. Once invested in capital markets, these resources become exposed to financially mediated risks. The guarantee limits the downside transferred to members, while random risk aversion prevents risk-bearing from being represented by a single preference type. These features connect the formal analysis to Marxist political economy's concern with social reproduction and the financialization of retirement provision [1–3, 10, 12]. In the context of Chinese modernization, this interpretation is consistent with the broader objectives of common prosperity, equitable risk-sharing, and sustainable social security. The model does not measure progress toward those objectives or evaluate the distributive performance of China's pension system. Such claims require institutional data on coverage, contribution burdens, benefit incidence, and redistribution [13]. Within this boundary, the framework provides a quantitative basis for studying prudent investment and risk governance in protected DC plans.

Author contributions

Yang Jiang: Conceptualization, methodology, formal analysis, investigation, visualization, writing–original draft. Yong He: Conceptualization, methodology, supervision, validation, writing–review and editing. Yulei Chen: Formal analysis, validation, visualization, writing–review and editing. All authors have read and approved the final manuscript.

Use of Generative-AI tools declaration

The authors used OpenAI ChatGPT/Codex during manuscript revision to assist with English language editing, reference format checking, and LaTeX formatting. The authors take full responsibility for the content of the manuscript.

Conflict of interest

The authors declare no competing interests.

References

1. K. Marx, *Capital: A Critique of Political Economy,* London: Princeton University Press, 1976.
2. I. Gough, *The Political Economy of the Welfare State,* 1 Eds., London: Red Globe Press, 1979. https://doi.org/10.1007/978-1-349-16122-5
3. I. Bakker, Social reproduction and the constitution of a gendered political economy, *New Polit. Econ.,* **12** (2007), 541–556. https://doi.org/10.1080/13563460701661561
4. K. Marx, *Critique of the Gotha Programme,* London: Lawrence & Wishart Progress Publishersin, 1989.

5. J. F. Boulier, S. Huang, G. Taillard, Optimal management under stochastic interest rates: The case of a protected defined contribution pension fund, *Insur. Math. Econ.,* **28** (2001), 173–189. https://doi.org/10.1016/S0167-6687(00)00073-1
6. G. Deelstra, M. Grasselli, P. F. Koehl, Optimal investment strategies in the presence of a minimum guarantee, *Insur. Math. Econ.,* **33** (2003), 189–207. https://doi.org/10.1016/S0167-6687(03)00153-7
7. N. Han, M. Hung, Optimal asset allocation for DC pension plans under inflation, *Insur. Math. Econ.,* **51** (2012), 172–181. https://doi.org/10.1016/j.insmatheco.2012.03.003
8. P. Boyle, M. Hardy, Guaranteed annuity options, *ASTIN Bull.,* **33** (2003), 125–152. https://doi.org/10.2143/AST.33.2.503687
9. A. J. G. Cairns, D. Blake, K. Dowd, Stochastic lifestyling: Optimal dynamic asset allocation for defined contribution pension plans, *J. Econ. Dyn. Control,* **30** (2006), 843–877. https://doi.org/10.1016/j.jedc.2005.03.009
10. B. Fine, Financialization from a Marxist perspective, *Int. J. Polit. Econ.,* **42** (2013), 47–66. https://doi.org/10.2753/IJP0891-1916420403
11. C. Lapavitsas, Financialised capitalism: Crisis and financial expropriation, *Hist. Mater.,* **17** (2009), 114–148. https://doi.org/10.1163/156920609X436153
12. P. Langley, In the eye of the perfect storm: The final salary pensions crisis and financialisation of Anglo-American capitalism, *New Polit. Econ.,* **9** (2004), 539–558. https://doi.org/10.1080/1356346042000311164
13. H. Zhu, A. Walker, Pension system reform in China: Who gets what pensions, *Soc. Policy Adm.,* **52** (2018), 1410–1424. https://doi.org/10.1111/spol.12368
14. S. L. Heston, A closed-form solution for options with stochastic volatility with applications to bond and currency options, *Rev. Financ. Stud.,* **6** (1993), 327–343. https://doi.org/10.1093/rfs/6.2.327
15. J. C. Cox, J. E. Ingersoll, S. A. Ross, A theory of the term structure of interest rates, *Econometrica,* **53** (1985), 385–407. https://doi.org/10.2307/1911242
16. J. Sun, Z. Li, Y. Li, Equilibrium investment strategy for DC pension plan with inflation and stochastic income under Heston's SV model, *Math. Probl. Eng.,* **2016** (2016), 2391849. https://doi.org/10.1155/2016/2391849
17. G. H. Guan, Z. X. Liang, Optimal management of DC pension plan in a stochastic interest rate and stochastic volatility framework, *Insur. Math. Econ.,* **57** (2014), 58–66. https://doi.org/10.1016/j.insmatheco.2014.05.004
18. L. Zhang, D. Li, Y. Lai, Equilibrium investment strategy for a defined contribution pension plan under stochastic interest rate and stochastic volatility, *J. Comput. Appl. Math.,* **368** (2020), 112536. https://doi.org/10.1016/j.cam.2019.112536
19. P. Wang, Z. Li, Robust optimal investment strategy for an AAM of DC pension plans with stochastic interest rate and stochastic volatility, *Insur. Math. Econ.,* **80** (2018), 67–83. https://doi.org/10.1016/j.insmatheco.2018.03.003
20. L. A. Grzelak, C. W. Oosterlee, On the Heston model with stochastic interest rates, *SIAM J. Financ. Math.,* **2** (2011), 255–286. https://doi.org/10.1137/090756119

21. G. Ascione, F. Mehrdoust, G. Orlando, O. Samimi, Foreign exchange options on Heston-CIR model under Lévy process framework, *Appl. Math. Comput.,* **446** (2023), 127851. https://doi.org/10.1016/j.amc.2023.127851

22. L. V. Ballestra, E. D'Innocenzo, A. Guizzardi, A new bivariate approach for modeling the interaction between stock volatility and interest rate: An application to S&P500 returns and options, *Eur. J. Oper. Res.,* **314** (2024), 1185–1194. https://doi.org/10.1016/j.ejor.2023.11.049

23. G. A. G. Alserda, B. G. C. Dellaert, L. Swinkels, F. S. G. van der Lecq, Individual pension risk preference elicitation and collective asset allocation with heterogeneity, *J. Bank. Finance,* **101** (2019), 206–225. https://doi.org/10.1016/j.jbankfin.2019.02.014

24. T. Bollerslev, M. Gibson, H. Zhou, Dynamic estimation of volatility risk premia and investor risk aversion from option-implied and realized volatilities, *J. Econom.,* **160** (2011), 235–245. https://doi.org/10.1016/j.jeconom.2010.03.033

25. J. Burgaard, M. Steffensen, Eliciting risk preferences and elasticity of substitution, *Decis. Anal.,* **17** (2020), 314–329. https://doi.org/10.1287/deca.2020.0415

26. S. Desmettre, M. Steffensen, Equilibrium investment with random risk aversion, *Math. Finance,* **33** (2023), 946–975. https://doi.org/10.1111/mafi.12394

27. T. Björk, A. Murgoci, A theory of Markovian time-inconsistent stochastic control in discrete time, *Finance Stoch.,* **18** (2014), 545–592. https://doi.org/10.1007/s00780-014-0234-y

28. T. Björk, M. Khapko, A. Murgoci, On time-inconsistent stochastic control in continuous time, *Finance Stoch.,* **21** (2017), 331–360. https://doi.org/10.1007/s00780-017-0327-5

29. L. Wang, B. W. Jia, Equilibrium investment strategies for a defined contribution pension plan with random risk aversion, *Insur. Math. Econ.,* **125** (2025), 103140. https://doi.org/10.1016/j.insmatheco.2025.103140

30. A. Friedman, *Partial Differential Equations of Parabolic Type,* New Jersey: Prentice–Hall, 1964.



AIMS Press

© 2026 the Author(s), licensee AIMS Press. This is an open access article distributed under the terms of the Creative Commons Attribution License (https://creativecommons.org/licenses/by/4.0)